Volume 27
Number 5
7 February 2025
Pages 1227-1578

Green Chemistry

Cutting-edge research for a greener sustainable future

rsc.li/greenchem

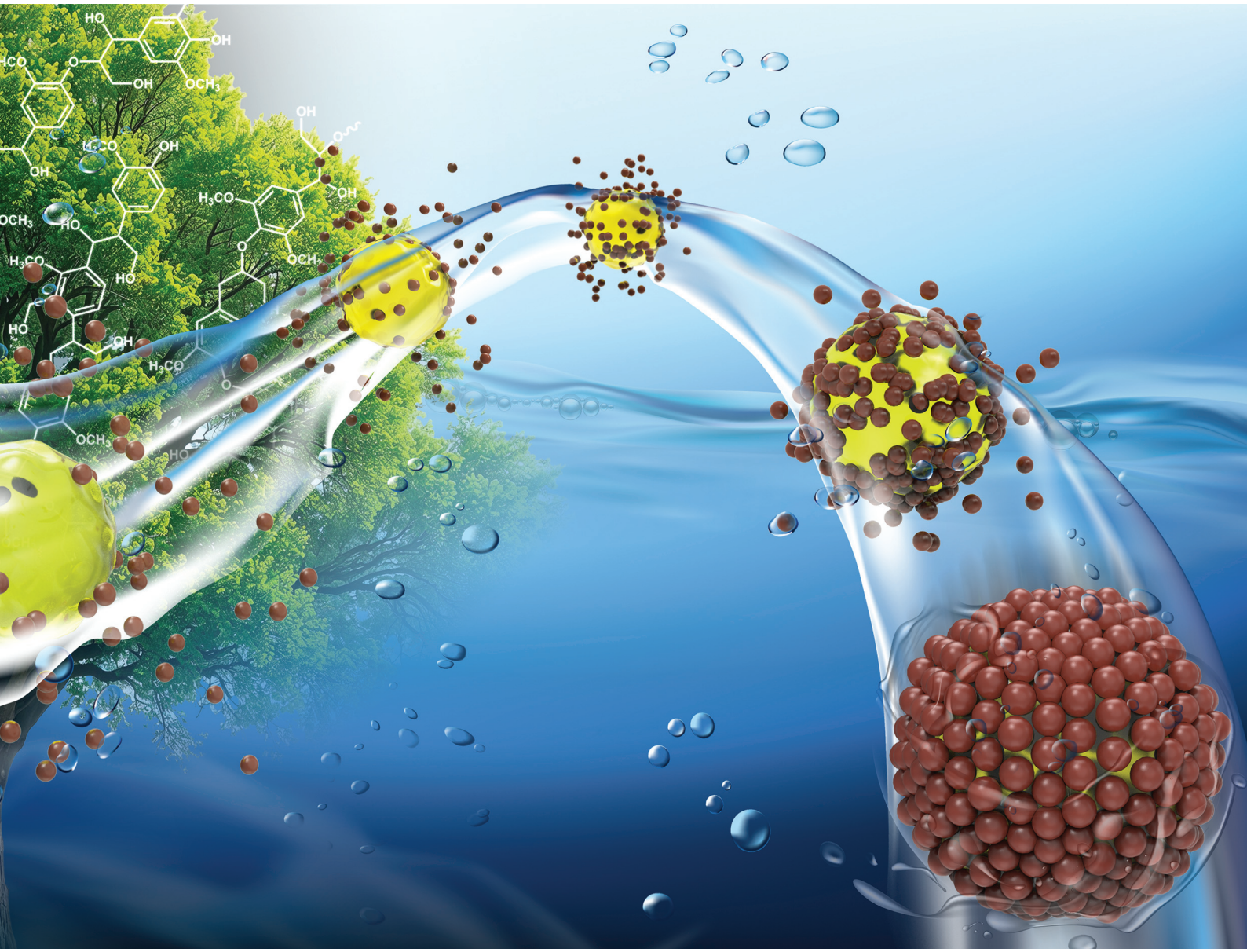

ISSN 1463-9262

ROYAL SOCIETY OF CHEMISTRY

TUTORIAL REVIEW

Caoxing Huang, Wenji Yu, Kai Zhang *et al.*

Pickering multiphase materials using plant-based colloidal lignin nanoparticles

25 YEARS ANNIVERSARY

Green Chemistry

TUTORIAL REVIEW

View Article Online
View Journal | View Issue

Cite this: *Green Chem.*, 2025, **27**, 1300

Pickering multiphase materials using plant-based colloidal lignin nanoparticles

Jian Gan, †[a,d] Yifei Zhan,†[b] Jing Fan,†[b] Jifu Wang,[c] Qi Gao,[d] Caoxing Huang,*[a] Wenji Yu*[a,d] and Kai Zhang *[b]

Received 8th November 2024,
Accepted 28th November 2024

DOI: 10.1039/d4gc05713a

rsc.li/greenchem

A Pickering emulsion, stabilized by amphiphilic solid particles, is a highly functional and stable system that has attracted significant research interest. Lignin, an amphiphilic biomacromolecule found widely in nature, can be transformed into nanoparticles using modern nanotechnology with great potential for use in Pickering emulsions. Despite numerous studies exploring the function of colloidal lignin particles (CLPs) in producing Pickering emulsions, there are few systematic reviews on the state-of-the-art works related to CLP-stabilized Pickering emulsions. In this review, we summarize recent advances in synthesis processes, formation mechanisms, structural characteristics and surface properties of CLPs on the stability and functionality of Pickering emulsion systems. We also highlight advanced applications of CLP-stabilized Pickering emulsions at present and propose future development directions for improving their synthesis technology using lignin as a stabilizer to enhance their properties. Our hope is that this review will serve as a roadmap for scientists engaged in research on CLP-Pickering emulsions across different scientific fields to achieve optimal material performance goals.

1. Introduction

Emulsions, which are inherently thermodynamically unstable systems, consist of two phases that are incompatible with each other. Surfactants are commonly used to effectively reduce the interfacial tension between these phases. This reduction in interfacial tension serves to decrease the overall free energy of the mixing system, thereby maintaining the dispersion stability of the constituent phases of the emulsion.[1] In contrast to conventional emulsions that rely on surfactants for stabilization, Pickering emulsions represent a distinct class of emulsion systems anchored in the utilization of solid particles (see Fig. 1). The earliest recorded instance of a Pickering emulsion can be traced back to 1904 when Ramsden made a pioneering discovery. He found that solid powder could form a dense particle coating on the surface of paraffin droplets, enabling even dispersion in water and subsequent formation of stable emulsions.[2] In 1907, following extensive research, Pickering offered a preliminary elucidation of the stabilization mechanism associated with this distinctive type of emulsion.[3] Subsequently, as researchers gained deeper insights, the stabilization mechanism of Pickering emulsions was gradually unveiled and clarified.[4,5]

However, the emulsion known as "Pickering emulsion" in honor of its inventor initially failed to garner widespread attention and did not incite international research fervor until the 21st century.[6,7] In comparison to conventional emulsions, Pickering emulsions stabilized by solid particles offer significant advantages such as low toxicity, versatility, high stability, and reduced emulsifier content,[8,9] and have been known and used in industrial polymerization.[10–12] Initially, research primarily focused on inorganic particles with silica particles designated as the "gold standard" Pickering stabilize, providing fundamental insights into the principles of Pickering emulsion stabilization.[13] Recently, colloidal science has entered a new era of Pickering stabilization by expanding its scope from simple inorganic materials to a diverse range of functional nanoparticles and micro-particles including magnetic nanoparticles, conductive particles, pH-responsive particles, and carbon nanotubes.[6,14] Notably, there has been an increasing emphasis on sustainability which has driven exploration into clean-label natural biopolymer particles specifically addressing the rising global demand for eco-friendly materials.[15] Consequently, extensive investigations have been conducted on various biomass nanoparticles such as cellulose nanofibers,[16–18] chitosan nano-

[a]*Co-Innovation Center of Efficient Processing and Utilization of Forest Resources, Nanjing Forestry University, Nanjing 210037, China. E-mail: hcx@njfu.edu.cn, chinayuwj@126.com*
[b]*Sustainable Materials and Chemistry, Dept. Wood Technology and Wood-based Composites, University of Göttingen, Büsgenweg 4, 37077 Göttingen, Germany. E-mail: kai.zhang@uni-goettingen.de*
[c]*Institute of Chemical Industry of Forest Products, Chinese Academy of Forestry, Nanjing, 210042, China*
[d]*Research Institute of Wood Industry, Chinese Academy of Forestry, Beijing 100091, China*
†These authors contributed equally to this work.

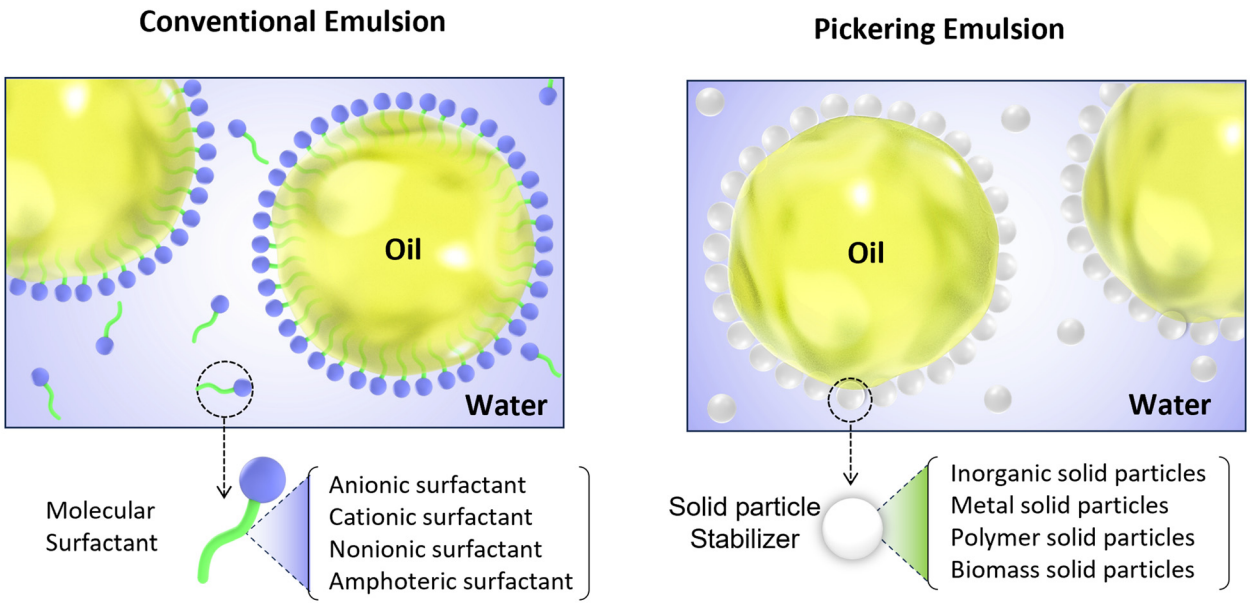

Fig. 1 The interface characteristics of traditional emulsion and Pickering emulsion.

particles, plant protein particles, and starch nanoparticles.[19–21] This transition aligns with the broader realm of colloidal science that encompasses a wide array of particle types aimed at satisfying the growing requirement for environmentally conscious and naturally sourced materials.[22]

Lignin is the second most abundant natural polymer derived from plants, following cellulose.[23] It possesses an aromatic composition with a three-dimensional spatial structure, consisting of numerous syringyl (S), guaiacyl (G), and *p*-hydroxyphenyl (H) units linked together by both ether and carbon–carbon bonds (Fig. 2).[24,25] This unique lignin structure contributes to several desirable properties, including sustainability, biodegradability, multiple active functional groups, cost-effective production, as well as antioxidant and UV-absorbent capabilities.[25,26] Consequently, lignin can be utilized as a functional material in the fabrication of composites such as thermoset resins, thermoplastics, foams, and adhesives through physical blending or cross-linking processes.[27]

However, the potential of lignin-containing composites as high-value materials is often limited by their rigid structure and the presence of a heterogeneous, polydisperse, and irregular morphology. In recent years, modern nanotechnology has emerged as a novel approach for efficient utilization of lignin. Lignin can be processed into spherical colloidal lignin particles (CLPs) through strong π–π interactions and hydrogen bonding.[28] Moreover, surface functionalization modifications can significantly expand its diverse range of applications.[29,30] Unlike macromolecular lignin, CLPs possess controllable particle sizes, uniform structures, and excellent dispersion properties.[31] These attributes have generated significant research interest in various fields such as catalysis, drug delivery, sterilization, hydrogel development *etc*. Particularly noteworthy are the nonpolar aromatic and polar hydroxy groups in lignin macromolecules that endow natural amphiphilicity to their particulate counterparts. Extensive investigations have been carried out regarding the functionality of CLPs as stabilizers within oil-in-water (O/W) Pickering emulsions. These emulsions exhibit remarkable dispersion stability, coupled with thermal resilience, salt resistance, and noteworthy pH-responsive characteristics. These attributes collectively present substantial promise for diverse applications, encompassing UV shielding, antioxidant formulations, and drug packaging among others.[32,33]

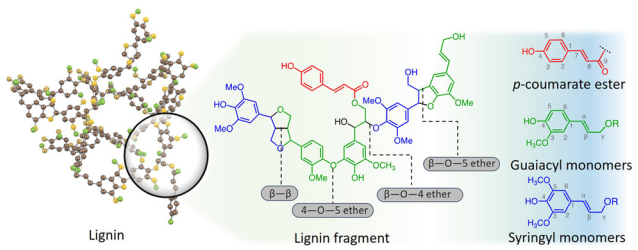

Fig. 2 The typical structure and constituent units of nature lignin.

However, there is currently a lack of a systematic review on the research related to Pickering emulsions stabilized by CLPs, particularly in terms of the preparation process of CLPs, the distinct types and forms of lignin, and their impacts on the properties and applications of Pickering emulsions. It is crucial to gain a comprehensive understanding of the formation mechanism of CLPs based Pickering emulsions. This knowledge will enable researchers to optimize synthesis conditions and parameters for tailoring the properties of CLPs-

Pickering emulsions. Such a concerted effort has the potential to enhance efficiency, cost-effectiveness, and accelerate the exploration of novel applications for CLPs-Pickering emulsions.

In this review, our focus is on the methods, formation mechanisms, properties, and applications of CLPs-Pickering emulsions. Firstly, we delve into the structure and properties of CLPs utilized in the preparation of Pickering emulsions, considering their preparation and modification processes. Subsequently, we provide a comprehensive overview of the characteristics, properties, and applications of various functional materials derived from CLPs-Pickering emulsions. Lastly, we present an outlook on the current challenges and opportunities in the field of CLPs-Pickering emulsions. The primary objective of this review is to consolidate and analyze research findings and advancements related to CLPs in Pickering emulsions. The main purpose of this review is to offer valuable insights for future innovative designs and applications involving CLPs-Pickering emulsions (Scheme 1).

2. Preparation process and formation mechanism of CLPs

Lignin exhibits an interconnected network structure composed of aromatic units, formed through the radical coupling of phenylpropanoid monomers—precursor hydroxy-cinnamic alcohols, specifically p-coumaryl, coniferyl, and synapyl.[34] Typically binding to hemicelluloses, lignin envelops cellulose in the primary and secondary cell walls of plant cells, establishing covalent bonds with cellulose.[35,36] This primary structure manifests as a highly branched and amorphous biomacromolecule with substantial molecular weight and polydispersity. The proportions of various lignin monomers and chemical bonds vary across sources, intensifying the challenge of precisely determining lignin's chemical structure.[37] Currently, the precise molecular structure of natural lignin remains unknown, and the predominant form of lignin is a byproduct of the pulping process in the paper industry, primarily harnessed for its thermal energy generation through combustion processes.[38,39]

Industrial lignin can be categorized into four types (Kraft, lignosulfonate, soda, and enzymatic hydrolysis lignin) based on various sulfur or sulfur-free processes in pulp manufacturing.[34,40] These lignins retain numerous active chemical sites, ensuring reactivity in chemical reactions.[41] However, the hydrophobic properties and complex physicochemical structure of lignin, including inter- and intra-molecular hydrogen bonding, impact its compatibility with host matrices. The functional properties of blends containing lignin depend significantly on the compatibility between lignin and the host matrices.[42–45]

Lignin's amphiphilic characteristic enables the facile formation of nanoparticles, thereby enhancing material homogeneity and reducing the impact of its structural intricacies on material properties. Additionally, it imparts nano-specific attributes, such as a substantial specific surface area, which broadens the applicability of lignin nanoparticles.[29,46] As shown in Fig. 3, several nano strategies have been developed for transforming lignin which include self-assembly, mechanical crushing, and interfacial crosslinking techniques.[47,48] The resulting nano-sized lignin exhibits diverse forms such as nanospheres, nanotubes, nano micelles, and nano capsules due to different shaping processes employed.[49–51] More detailed information regarding these methods for producing CLPs is provided below.

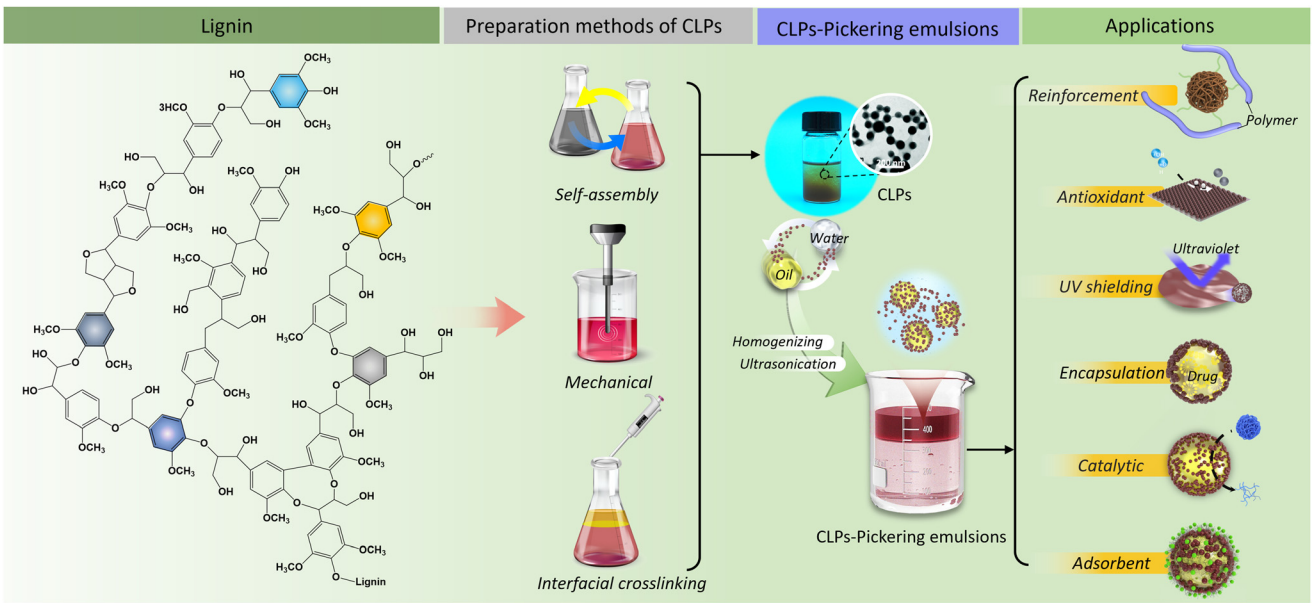

Scheme 1 Illustration of the overview of this review.

2.1. Self-assembly method

Self-assembly refers to the spontaneous formation of an ordered or organized structure in the absence of external influences, driven by specific non-covalent intermolecular interactions such as hydrophobic forces, electrostatic interactions, hydrogen bonding, and van der Waals forces.[52] However, in the case of CLPs, the concept of "self-assembly" cannot be precisely defined as a standalone method since it is always accompanied by other indirect methods. In other words, various techniques can induce the self-assembly process of CLPs.

2.1.1. Antisolvent self-assembly. As shown in Fig. 3a and 4, the antisolvent self-assembly method exploits the amphiphilic nature of lignin, characterized by a hydrophobic skeleton (*e.g.*, phenylpropane) and hydrophilic functional groups such as hydroxyl and carboxylic groups. In this process, an excess of antisolvent is introduced to an organic solvent solution containing lignin. This addition triggers the hydrophobic effect of lignin, resulting in its self-assembly precipitation and the formation of CLPs. This approach is also known as the antisolvent precipitation method.[53,54]

In polar solvents, the hydrogen bond network of lignin, both inter-molecular and intra-molecular, undergoes disruption. This results in the self-assembly of hydrophobic regions of lignin into the core of CLPs through hydrophobic interactions, while exposing the hydrophilic regions on the surface.

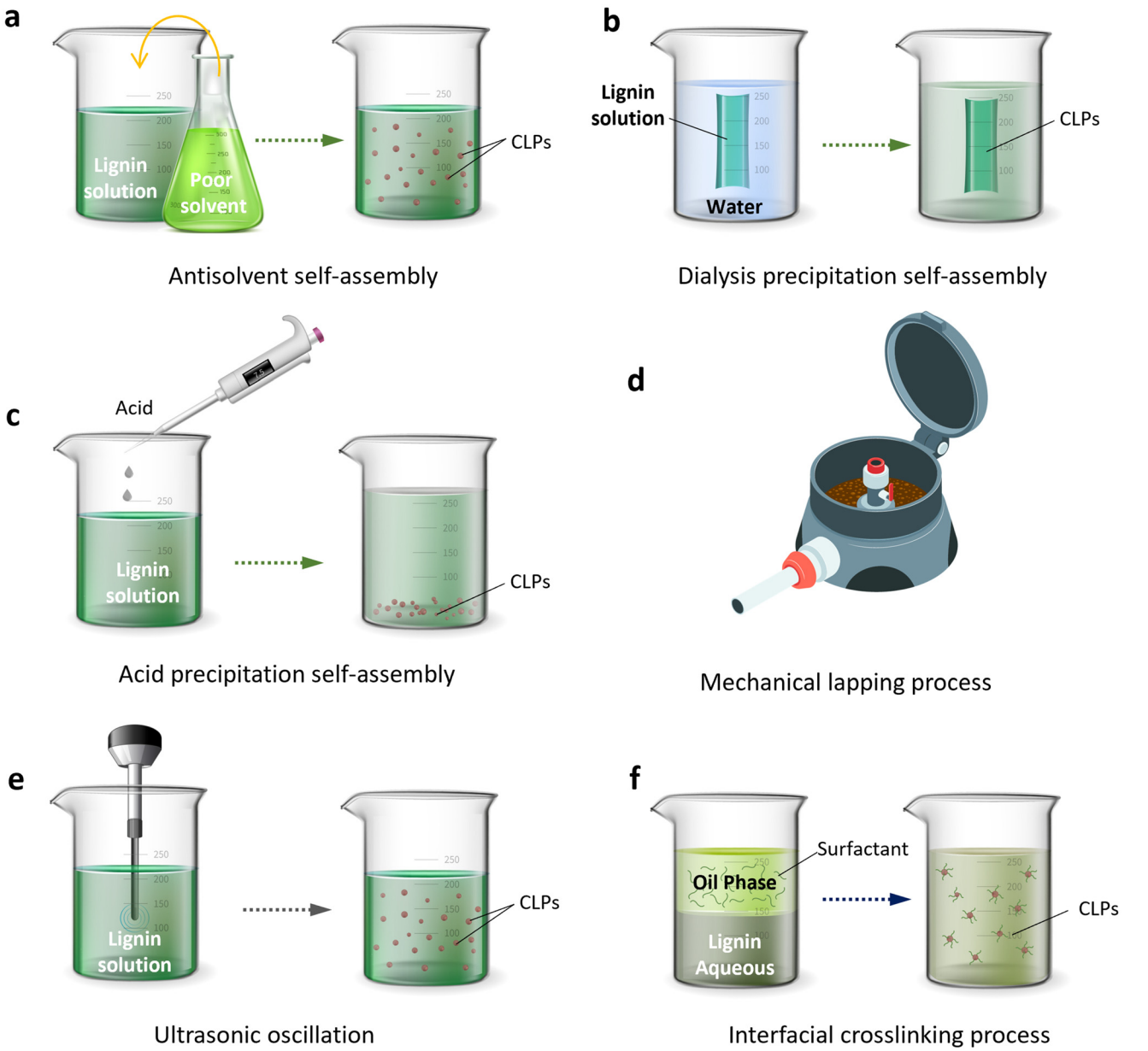

Fig. 3 Preparation methods of CLPs. Antisolvent self-assembly of CLPs (a); dialysis precipitation self-assembly of CLPs (b); acid precipitation self-assembly of CLPs (c); mechanical lapping process of CLPs (d); ultrasonic oscillation of CLPs (e); interfacial crosslinking process of CLPs (f).

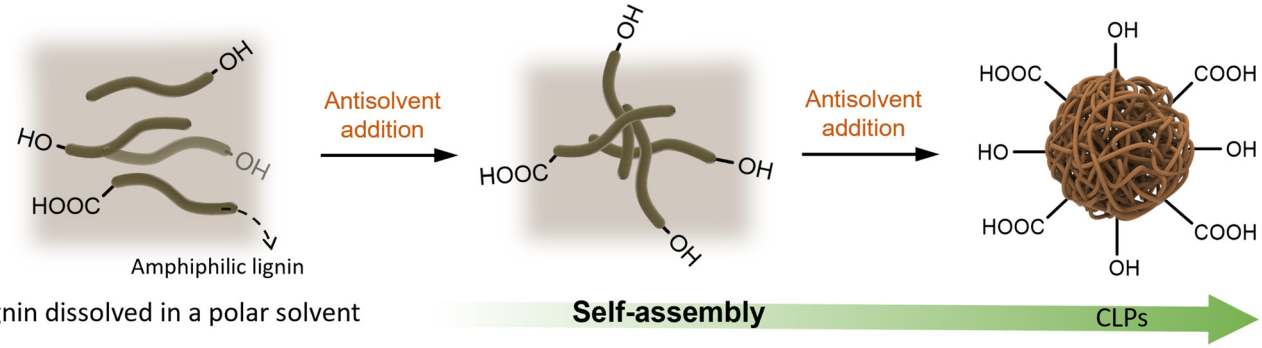

Fig. 4 A schematic proposal for the formation of CLPs by self-assembly.

Upon introduction to water, non-covalent interactions such as hydrogen bonding between surface hydroxyl groups facilitate the formation of hydrophilic aggregates. Consequently, lignin tends to aggregate into spherical nanoparticles in order to minimize contact with the non-solvent phase and maximize its surface area.[55]

However, relying solely on hydrophobic interactions proves insufficient to overcome repulsive forces between charged lignin molecules. Hence, it has been proposed that non-bonding orbital interactions among aromatic components of lignin molecules drive their association.[56] The strong π-stacking interaction leads to a reduction in energy levels of electrons in CLPs as evidenced by ultraviolet absorption spectra analysis.[57,58] There is a shift in absorption peak from 280 nm (lignin nanospheres in THF) to 284 nm (lignin nanospheres in water).[59] This shift is attributed to π–π transitions within guaiacyl groups present in CLPs. During the self-assembly process, the strong hydrophobic nature of the lignin phenylpropane structure prompts the movement of lignin molecules as water molecules are introduced. This movement results in the formation of a film at the interface between the organic phase and the water phase. As the proportion of water phase increases, the pressure gradient inside and outside the lignin molecule membrane intensifies, leading to the gradual penetration of water molecules into the membrane.[53] Lignin molecules with pronounced hydrophilicity progressively accumulate on the inner surface of the membrane through π–π interactions.[60] Simultaneously, the internal and external pressure gradient continues to grow until the organic phase is entirely removed, ultimately yielding stable lignin nanospheres.[33,57] CLPs prepared using the reverse addition sequence typically exhibit larger particle sizes than those produced when the water phase is added to the organic phase. The size difference can be attributed to the increased precipitation rate resulting from the abrupt change in internal and external pressure during the addition of the organic phase to the water phase.[61,62] Various solvent systems, such as tetrahydrofuran/water, ethanol/water, acetone/water,[63,64] and dioxane/cyclohexane, have been extensively developed and applied in nanolignin preparation. In these studies, the primary driving force behind CLPs self-assembly is attributed to π–π interaction.[55]

In addition, a more comprehensive understanding of the distinctions between different solvent systems is still necessary.[61] In the study conducted by Chen *et al.*,[65] an extensive investigation was carried out to elucidate the influence mechanism of solvent diversity on CLPs formation. Their findings suggest that the solvation of various organic solvents plays a crucial role in CLPs formation. This research focused on lignin model compounds and revealed three distinct configurations resulting from three interactions (π–π, CH–π, and no interaction) within the molecule: accumulation, lateral movement, and stretching behaviors. The study indicated that lignin molecules adopting a biased stack conformation in the solvent were more prone to self-assemble through intermolecular π–π interactions while being surrounded by solvent molecules forming stacked gum clusters. On the other hand, lignin molecules exhibiting lateral moving and stretching conformations may face difficulties in tightly clustering due to occupying molecular space already occupied by solvent molecules. Solvents such as DMF and DMSO disrupt lignin's intramolecular π–π packing behaviours, hindering the self-assembly process due to strong solvation effects. Additionally, methanol or acetone partially disrupts π–π accumulation leading to only a small number of nanoparticles being formed. In contrast, GVL and THF effectively maintain π–π packing within the molecule resulting in high-yield nanospheres.[65]

In summary, the reversed-solvent precipitation method emerges as the predominant technique for CLPs preparation, deeply rooted in the fundamental composition and properties of lignin. The hydrophobicity of lignin molecules is intricately associated with van der Waals forces and π–π interactions.[56] The driving force behind the self-assembly process of lignin is believed to vary in different environments, with the potent π–π interaction recognized as the primary force shaping CLPs formation. The hollow structure of CLPs is attributed to the presence of phenol hydroxyl groups. A higher content of phenol hydroxyl groups strengthens intermolecular hydrogen bonding and electrostatic forces, thereby weakening the compact structure formed by π–π interaction of CLPs and ultimately leading to a hollow structure.[55] Furthermore, CLPs prepared through traditional solvent exchange methods exhibit an initial negative charge of approximately 30 mV and remain stable in the

short term. However, over time, ionic species present in media neutralize the surface charge of nanoparticles, resulting in CLPs aggregation or even precipitation. This poses a critical challenge that needs to be addressed for their sustained retention and widespread large-scale application.[66]

2.1.2. Dialysis precipitation self-assembly. The dialysis precipitation self-assembly method is an extension of the solvent precipitation self-assembly technique, which involves dissolving lignin in organic solvents and introducing a poor lignin solvent through dialysis to facilitate lignin self-assembly (Fig. 3b). Solvent exchange and the self-assembled precipitation of lignin are achieved by utilizing the solvent pressure difference between the inside and outside of the semi-permeable membrane.[46] The selective penetration of the semi-permeable film results in a continuous and slow rate of solvent exchange, creating a consistent and uniform driving force for self-assembly.[67] Consequently, dialysis precipitation can yield CLPs with a stable concentration distribution, unlike solvent exchange precipitation. Bertolo *et al*. highlighted that the water displacement to the good solvent in the direct dialysis process occurs gradually and at a slow pace, leading to a sluggish self-assembly of lignin macromolecular structure in water.[67] Conversely, in the solvent transfer method, there is an abrupt and rapid displacement of water to good solvent, preventing sufficient time for normal self-assembly of lignin macromolecules in water. These disparities may account for the higher hydrophilicity observed in CLPs obtained through solvent transfer compared to those obtained *via* direct dialysis.

However, chemical modification of lignin is often necessary to enhance its solubility in solvents during the dialysis self-assembly process. In a study conducted by Miikka Lievonen *et al*.,[68] it was observed that higher concentrations of lignin solution led to larger pressure differences between the inside and outside of the semi-permeable membrane, resulting in faster nucleation and growth rates during the self-assembly process. This increased availability of lignin within the system for nanoparticle growth made it more susceptible to variations in particle size during lignin particle formation. Therefore, strict control over production processes is often required when using dialysis precipitation methods to prepare lignin nanoparticle, ensuring nanoparticles with regular morphology and uniform size.

2.1.3. Acid precipitation self-assembly. The acid precipitation self-assembly method induces the precipitation and self-assembly of lignin to form nanoparticles by lowering the pH value of an organic solution or alkaline aqueous solution containing dissolved lignin, thereby reducing the solubility of lignin in an acidic environment (Fig. 3c).[69] The majority of studies on acid precipitation self-assembly of lignin solutions have primarily focused on kraft lignin, which represents the most extensively processed and industrially produced type of lignin, as well as lignosulfonate, the most commercially utilized source of lignin.[70,71] In an aqueous solution, sulfonated lignin becomes soluble in an alkaline medium through ionization of phenolic hydroxyl groups. In 1979, Lindstrom conducted a study on the association and precipitation behavior of kraft lignin in aqueous solutions with varying pH levels ranging from 8.6 to 3.7.[72] It was observed that the degree of association between lignin molecules increased as carboxyl group ionization in lignin decreased. Consequently, this study suggested that hydrogen bonds formed between carboxyl groups and various ether oxygen and hydroxyl groups triggered the association between lignin molecules.

However, numerous studies have indicated that hydrogen bonding is not considered the primary driving force behind the association of lignin in high-concentration solutions. The morphology and size changes of nano lignin are directly influenced by pH value.[73] Research demonstrates that as the pH value decreases, the π–π interaction and hydrophobicity of lignin molecules are enhanced, facilitating lignin accumulation. However, excessive acidity can reduce the surface negative charge of lignin particles, resulting in decreased stability. Ma *et al*. utilized the acid precipitation method to obtain CLPs with uniformity, excellent dispersion,[66] controllable size, and long-term stability (no apparent size change or particle precipitation observed in aqueous solution for 90 days) directly from black liquor. The improved stability of CLPs is primarily attributed to their hydrophilicity and high content of negatively charged hemicellulose. The study also observed a gradual decrease in particle size and theta potential on the surface of CLPs with decreasing pH value.

2.2. Mechanical method

The preparation of CLPs through mechanical methods primarily involves the application of external forces, such as ultrasonic waves and mechanical grinding, resulting in their size reaching or approaching the nanometre scale. In comparison to the self-assembly method, the mechanical approach eliminates the need for organic solvents, thereby offering advantages in terms of cost-effectiveness and environmental friendliness.

2.2.1. Mechanical lapping. The method of utilizing mechanical grinding to externally degrade lignin and prepare CLPs is referred to as the mechanical grinding method. Nair *et al*. employed a high shear homogenizer to mechanically shear cowhide lignin and investigated the size distribution of lignin particles under different durations of mechanical shearing forces (Fig. 3d).[74] The results revealed that after 4 hours of mechanical treatment, the size distribution of CLPs primarily ranged from 20–30 nm, demonstrating enhanced uniformity compared to the original lignin particles (mainly 0–5 μm). Furthermore, analysis using ^{13}C NMR and ^{31}P NMR indicated that there were no changes in the chemical composition and structure of lignin before and after mechanical treatment.

Leonidas Matsakas *et al*. utilized steam explosion fractionation with mixed organic solvents to separate birch flakes from lignin at varying ethanol contents.[75] They employed homogeneous shear method in ethanol solutions with different volume fractions for preparing CLPs. Fourier infrared spectroscopy demonstrated that during the homogeneous shear process, there was no chemical modification or decomposition occurring in the composition of CLPs. The only influence observed was on their size and uniformity due to variations in

ethanol content. In the study conducted by Yaqoob *et al.*,[76] the homogenization method was employed to reduce lignin into nanoparticles, with four different shear speeds (*i.e.*, 6400, 8400, 10 400, and 12 400 rpm) investigated for controlling the particle size of lignin. Notably, the highest speed of homogenizer yielded nanoparticles with superior size distribution and favourable zeta potential value.

In summary, this environmentally friendly mechanical method eliminates the need for organic solvents making it suitable for large-scale applications. This promotes research on applying lignin nanoparticle in various fields such as food industry, medicine, and healthcare sectors. However, it should be noted that CLPs prepared using this method currently exhibit poor structural and dimensional stability which limits their mature application in industrial production.

2.2.2. Ultrasonic oscillation. The ultrasonic crushing method involves subjecting the lignin solution to ultrasound treatment in order to disrupt the molecular chain, utilizing micro-bubble rupture caused by the transient state of local high pressure and temperature formed during and after ultrasound (Fig. 3e). This process aims to reduce the size of large lignin particles and obtain CLPs. In a study conducted by Gilca *et al.*, CLPs were prepared using physical ultrasonication.[77] The mechanical ultrasonic preparation of CLPs involves two distinct reaction modes: depolymerization of lignin side chains and oxidative coupling/polymerization, with depolymerization being the predominant mode. The study suggests that the depolymerization of lignin can be adjusted by modulating ultrasonic irradiation time or power.[78] Yin *et al.* dissolved switchgrass lignin in an alkaline solution and prepared CLPs using the ultrasonic method.[79] The study demonstrated that sulfonated groups were produced through the reaction between klaxon lignin and sodium hydroxide, resulting in obtained CLPs exhibiting a negative zeta potential of −33.1 mV. Agustin *et al.* directly prepared CLPs from sulfur-free alkaline pulping through acid precipitation and ultrasonic treatment without requiring drying or dialysis steps.[69] The preparation process enabled obtaining spherical nanoparticles with a layered structure and a negative surface charge within just 5 minutes of ultrasonic treatment. This method offers significant advantages such as reducing acid consumption significantly while enabling direct preparation of CLPs from highly concentrated lignin solutions.

2.3. Interfacial crosslinking process

The interfacial crosslinking process involves dissolving lignin and other monomers or polymers with diverse functional groups in two immiscible solvents. As shown in Fig. 3f and 5, this process typically entails the emulsion inversion reaction at the interface of the two solutions when one solution is dispersed into the other. The method serves to stabilize, generate particles, and form capsules.[80]

In this process, the lignin chain must undergo crosslinking induction to render it amphiphilic, enabling its dissolution in an alkaline solution to form a dispersed phase and in a solvent with surfactants. In the second step, a water–oil microemulsion is prepared, and the dissolved lignin is emulsified to facilitate lignin crosslinking at the oil–water interface. The addition of crosslinking agents during the emulsification process, often mediated by ultrasound, can enhance the crosslinking reaction of lignin.[80] The interfacial crosslinking method allows for the production of spherical micro and nano lignin particles as well as spherical micro/nano lignin capsules, modified lignin particles with high porosity, and composites with CLPs.

Wang *et al.* conducted a study where they synthesized carboxymethylated lignin in aqueous solution using nucleophilic substitution methods. They combined this with a small amount of alkyl polyglycoside as a macromolecular surfactant to stabilize a high internal phase emulsion loaded with 87% curcumin under neutral conditions. The capsule shell formed by carboxymethyl enzymatic hydrolysis lignin exhibited excellent anti-ultraviolet properties in their study. In another study by Wang *et al.*, sodium lignosulfonate rich in sulfonic and carboxyl groups was dissolved in water. Mixed surfactants with opposite charges were introduced into the system while adjust-

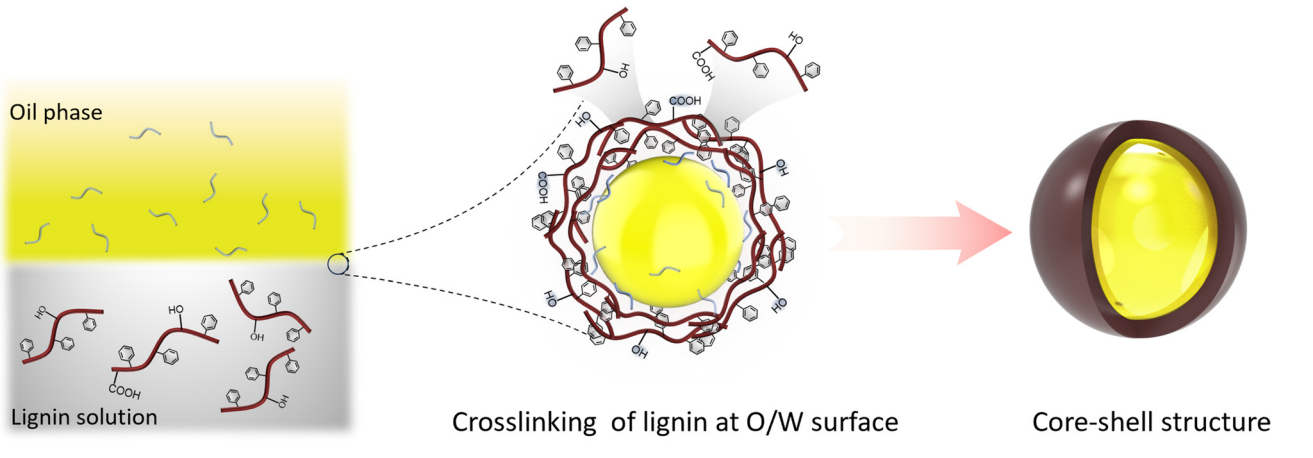

Fig. 5 A schematic proposal for the formation of CLPs by interfacial crosslinking process.

ing the action of lignin and mixed surfactants through non-ionic surfactants tritonX-100 and NaCl. This resulted in successful construction of CLPs consisting of rigid solid microspheres or hollow packages using interfacial crosslinking method. The interfacial crosslinking method demonstrated its applicability for rapidly preparing lignin spherical micro/nano capsules which showcased potential applications in biomedicine for encapsulating hydrophobic compounds and drug protection.

2.4. Other methods

As research progresses in the field of lignin nanotechnology, various methods have been explored for the preparation of CLPs, including the aerosol method. The aerosol method is a high-flux technique for preparing nano-sized lignin particles, which involves circulating a gas carrier containing a solution of lignin through a high-temperature heat pipe. This facilitates rapid drying and aggregation of lignin, followed by downstream collection of CLPs. By adjusting parameters such as the source of lignin, precursor concentration, atomization, and drying, the aerosol flow reactor method allows for one-step production of CLPs with uniform size and controllable properties. Ago *et al*. have successfully utilized aerosol spray technology to synthesize lignin particles with adjustable sizes and hydrophilicity, thereby demonstrating their ability to create stable Pickering emulsions.[84]

The advantages offered by aerosol technology include absence of liquid by-products, simple particle collection process, low-cost implementation, reduced number of processing steps required, continuous operation capability, and high product yield potential. Other synthesis methods that have been explored include controlled evaporation of atomized droplets containing lignin solution-circulating flash precipitation,[92] microbial degradation,[93] enzyme decomposition,[94] ice separation,[95] and CO_2 anti-solvent techniques.[96] However, these alternative approaches are yet to overcome challenges related to cost, stability and large-scale production.

Table 1 summarizes the particle sizes and morphologies of CLPs prepared from different lignin precursors under different processes. While the antisolvent method remains the primary process for preparing lignin nanoparticle, it faces challenges concerning solvent consumption and recovery, environmental safety, nanoparticle stability, and yield.[50] The selection of a suitable solvent is crucial in determining the production cost of cellulose CLPs. Green and simplified processes are increasingly advocated, with dialysis precipitation emerging as a notable method for producing CLPs with adjustable sizes; however, its scalability is limited due to expensive dialysis equipment. Mechanical methods such as ultrasonic crushing or mechanical grinding offer high efficiency, yield, and cost-effectiveness but present difficulties in controlling the quality of CLPs.[77] Biological methods encounter issues related to CLPs yield, enzyme production costs, and solvent usage. Consequently, further research is needed to promote and develop environmentally friendly large-scale processes for CLPs preparation.

3. Effect of CLPs properties on Pickering emulsions

At the two-phase interface, oil and water are typically immiscible due to the presence of strong interfacial tension. In Pickering emulsions, CLPs function as emulsifiers, reducing the tension between the two interfaces and promoting homogeneous mixing of the two phases. In emulsion technology,

Table 1 Summary of the synthesis of CLPs from various approaches

Lignin species	Preparation methodology	Particle dimension/nm	Morphology	Ref.
Enzymatic hydrolysis lignin	Acid precipitation self-assembly	48.9 ± 16.4	Spherical	81
Lignosulfonate	Antisolvent self-assembly	55 ± 26 and 86 ± 29	Spherical and hollow nanospheres	82
Alkali lignin	Acid precipitation self-assembly	20–100	Surface collapse	83
Kraft lignin and alkali lignin	Aerosol spray technology	>30	Spherical	84
Sodium lignosulfonate	Interfacial crosslinking process	100–400	Nanocapsules	85
Acid precipitation self-assembly	Antisolvent self-assembly	200	Spherical	54
Kraft lignin	Dialysis precipitation self-assembly	>300	Spherical	68
Kraft lignin	Antisolvent self-assembly	97	Spherical	86
Alkaline lignin	Acid precipitation self-assembly	182	Spherical	87
Kraft lignin	Antisolvent self-assembly	100	Spherical	88
Alkaline lignin	Antisolvent self-assembly	120–150	Spherical	65
Kraft lignin	Ultrasonic oscillation	39–185	Hollow and solid particle	55
Depolymerized lignin	Ultrasonic oscillation	237–539	Spherical	89
Kraft lignin	Ultrasonic oscillation	10–50	Sheet structure	78
Lignin	Acid precipitation self-assembly	>500	Irregular shape	71
Kraft lignin	Dialysis precipitation self-assembly	259 ± 4–274 ± 5.3	Spherical	90
Kraft lignin	Interfacial crosslinking process	27.4 ± 12.8–127.8 ± 43.6 μm	Spherical	91
Kraft lignin	Homogenization processes	250–1000	Spherical	75
Softwood kraft lignin	Antisolvent self-assembly, acid precipitation self-assembly with ultrasonic oscillation	87–125	Sheet structure	61
Hardwood birch lignin		112.5–187	Irregular spherical	
Soda lignin		90–150	Spherical	

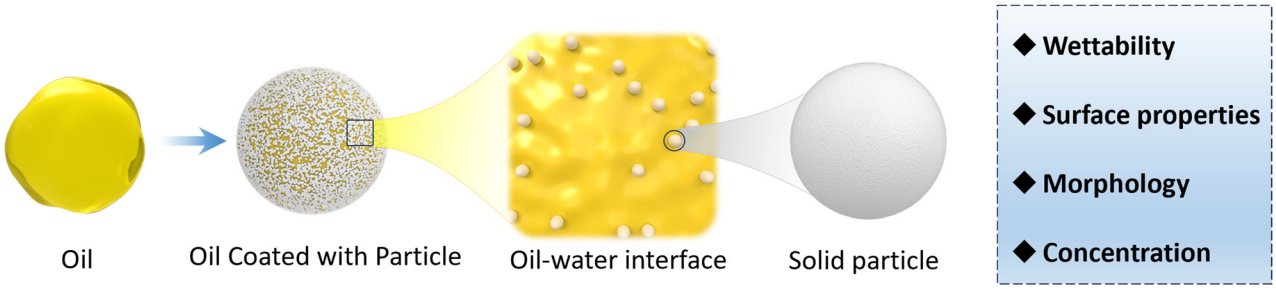

Scheme 2 The existence state and properties of nanoparticles at the interface of Pickering emulsion.

the stability of an emulsion is a critical factor for any application, which can be determined by observing a longer time required for phase separation (Scheme 2).[97] The study of Pickering emulsion stability encompasses essential physical properties such as nanoparticle type, droplet size, particle size distribution, and level of emulsion formation.[73] Among these factors, CLPs play a pivotal role in directly influencing the quality of the emulsion and its other physical properties including particle size and distribution. The impact of CLPs on the emulsion can be summarized by examining particle wettability, morphology, surface chemical properties, and concentration.

3.1. Wettability of CLPs

The assessment of CLPs' surface wettability is a critical factor in evaluating the stability of lignin particles at the oil–water interface. Within the nature lignin structure, a stable and intricate three-dimensional network carbon skeleton is formed by C6 and C3, establishing a hydrophobic nature. Concurrently, hydrophilic groups such as hydroxyl and carboxyl are distributed within the interior and at the ends of the skeleton. This dual distribution imparts a two-phase affinity to natural lignin, with a stronger hydrophobicity compared to hydrophilicity.

The surface wettability of CLPs can be characterized by the three-phase contact angle (θ_{OW}) at the oil–water interface, as illustrated in Fig. 6a. When $\theta_{OW} < 90°$, it indicates a stronger hydrophilicity, facilitating the formation of an "oil-in-water" (O/W) emulsion. Conversely, if $\theta_{OW} > 90°$, it signifies stronger lipophilicity, promoting the formation of a water-in-oil (W/O) emulsion (Fig. 6b and c). When θ_{OW} approaches 90°, it suggests a balanced hydrophilic–lipophilic character, contributing to superior interfacial stability and fostering the creation of a highly stable Pickering emulsion. To achieve a balanced two-phase affinity of lignin, it is essential to decompose the carbon skeleton, thereby releasing its polar groups. This process plays a crucial role in harmonizing the interaction between lignin particles and the interface, ensuring the stability of lignin particles in diverse conditions.

Lignin is known to be partially soluble in good solvents with high hydrogen-bonding capacity, such as ethanol, or moderately high polarity, such as acetone, THF and DMF.[98] The deconstruction and recombination of lignin can be effectively achieved through the selective dissolution of lignin in different solvents, leading to a reduction in the surface heterogeneity of macromolecular lignin.[99] Tian *et al.* utilized a binary mixed solvent composed of water and THF to fractionate CLPs with diverse surface wettability. The differentiation in surface

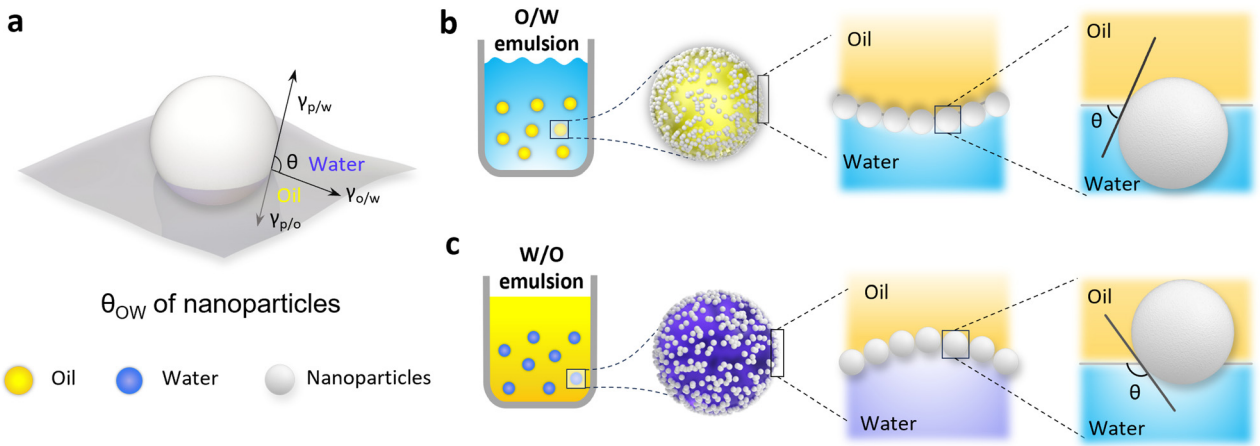

Fig. 6 Schematic diagram of three phase contact angles at the oil–water interface of nanoparticles (a); the oil-in-water (O/W) Pickering emulsion (b) and water-in-oil Pickering emulsion (c) stabilized by nanoparticles.

properties was determined by considering the interaction of molecular weight, particle size, and hydrophilic groups.[55] As a result, the θ_{ow} of these CLPs exhibited distinct hydrophilic characteristics at 13°, 136°, and 109°, respectively.[55] In Gao *et al.*'s study,[63] CLPs were synthesized from enzymatically hydrolyzed lignin powder using the acetone and water co-solvent method. In comparison with the original lignin, the θ_{ow} of CLPs at the oil–water interface decreased from 141° to 89°. The change in wettability primarily was attributed to the roughness variation, which is also related to the variation of the sizes and size distributions of the constituting particles (Fig. 7).

During the self-assembly process of lignin to form nanoparticles, alterations in solution polarity serves as a trigger for the self-assembly process of lignin. In response to strong polar bonding, the hydrophilic groups of lignin tend to preferentially orient themselves towards the polar environment, while the hydrophobic carbon skeleton congregates in the interior of the formed CLPs. As illustrated in Fig. 8a, this selective arrangement of lignin components within the nanoparticles is driven by the interplay of non-covalent bonds among lignin molecules, including hydrogen bonds, hydrophobic forces, and π–π stacking, leading to a distinct organization of hydrophilic and hydrophobic elements during the self-assembly process. Additionally, lignin molecules with higher hydrophilicity have a propensity to aggregate, leading to the formation of smaller-sized nanoparticles under the influence of hydrophobic forces. As CLPs undergo assembly and growth, the particle size gradually increases, accompanied by a reduction in the uniform distribution of functional groups on the particle surface. This phenomenon influences the surface wettability of CLPs, as the evolving structure and size of the particles modify the interaction between the surface and the surrounding environment.

Moreover, the protonation and deprotonation of lignin represents a classical method for regulating the surface wettability of CLPs through surface charge (Fig. 8b). Nasim Ghavidel observed that at pH 11, the functional groups on the surface of CLPs undergo deprotonation, resulting in a θ_{ow} at the oil–water interface of less than 20°, indicating superhydrophilicity.[100] Conversely, at pH 3, the θ_{ow} increases to 50°. Comparable results were obtained in the study of Tian *et al.*, who investigated the surface wettability of CLPs derived from dissolving Kraft lignin under varying pH conditions. The three-phase contact angles were measured at 36°, 75°, and 118° for pH values of 11, 7, and 2, respectively. These results suggest that Kraft CLPs (KLP) could serve as an effective emulsifier for Pickering emulsions. The change in pH value leads to

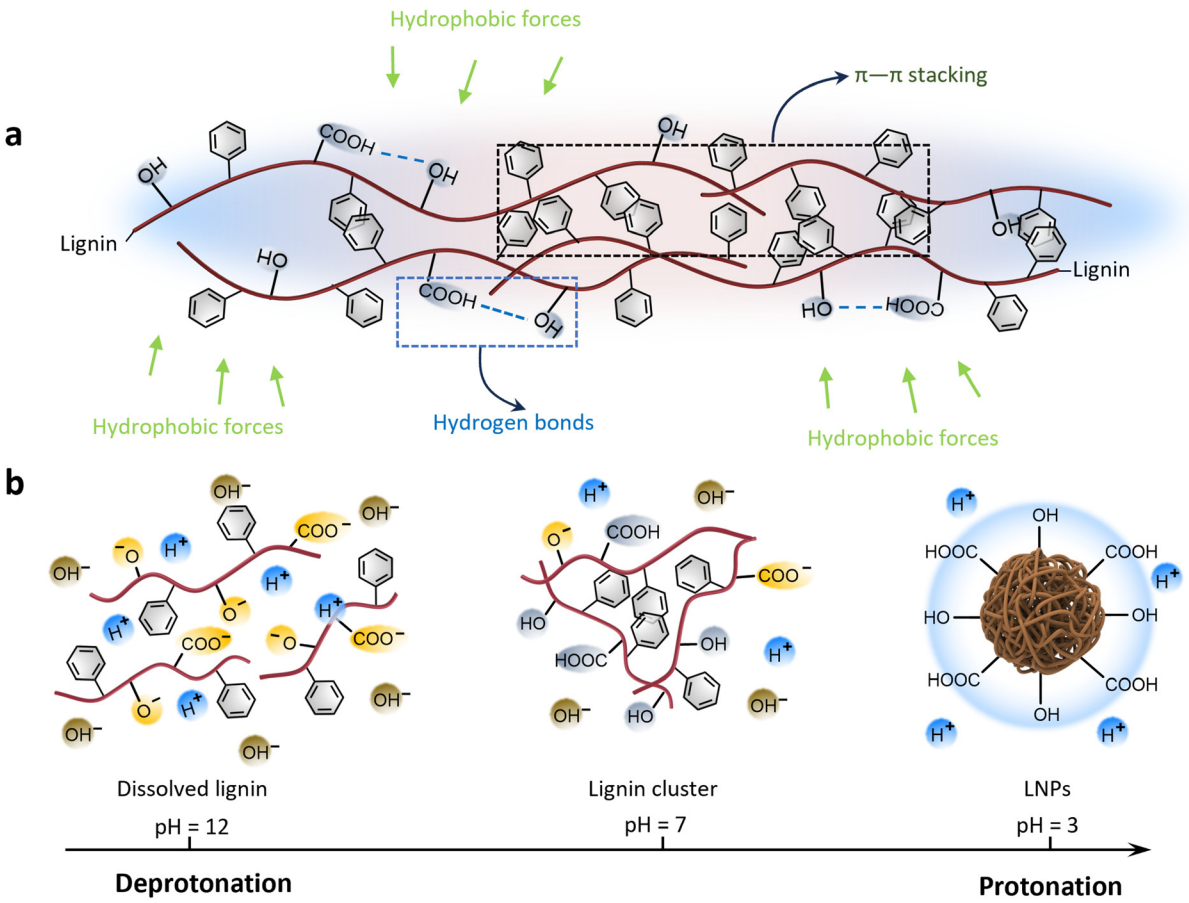

Fig. 7 The driving force of lignin in the self-assembly process (a); protonation of lignin as pH decreases during acid precipitation self-assembly (b).

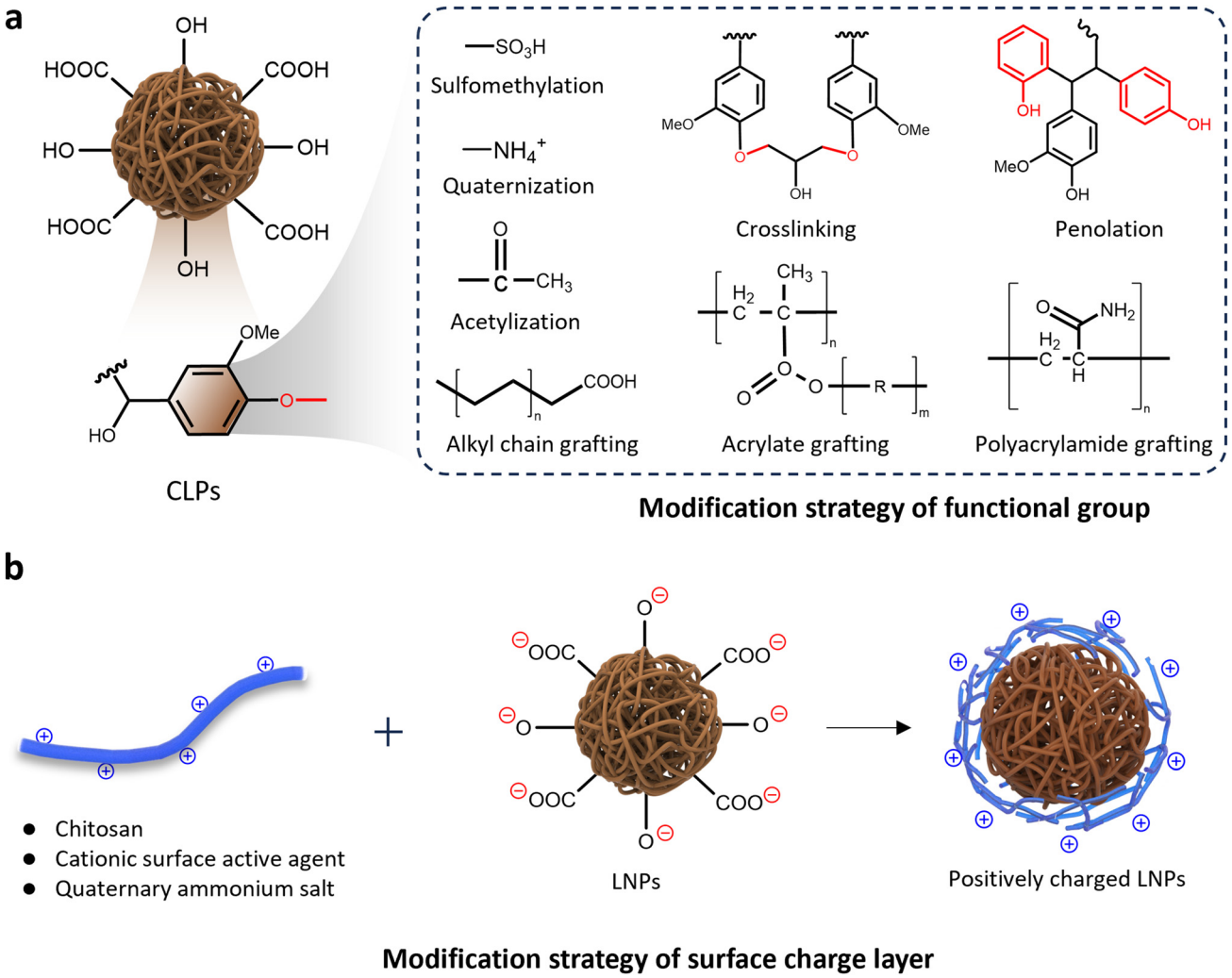

Fig. 8 Surface chemical modification strategy (a) and surface charge modification strategy (b) of lignin.

the protonation and deprotonation of functional groups of the CLPs. Studies indicate that the pK_a of the carboxylic and phenolic groups is about 4.7 and 9–10, respectively; these anionic groups are mostly deprotonated in alkaline media. At a pH > 11, lignin molecules are present mainly as hydrocolloids. As the pH decreases, the electrostatic repulsion between lignin molecules diminishes, leading to lignin molecules being predominantly present as both particles and hydrocolloids. When the environment is highly acidic (pH < 3), CLPs are formed due to the groups are dominantly protonated and the strong association strength of the lignin macromolecules. The absence of electrostatic repulsion between CLPs usually results in a compact and dense structure.

Caroline Hadjiefstathiou *et al.* investigated the interfacial tension generated by lignin micelles and colloidal particles at varying pH levels.[101] As the pH decreases, the quantity of soluble lignin micelles in the solution diminishes, resulting in a gradual increase in interfacial tension. In the established emulsion system, the competitive adsorption of different forms of lignin in the continuous aqueous phase can alter the emulsion's stability, fostering diverse rates and degrees of aggregation. This process gives rise to two states: Pickering stabilization and non-Pickering stabilization in the emulsion. The synergistic mechanism, characterized by a balanced presence of lignin particles and lignin micelles, was considered to contributes to the heightened stability of O/W emulsions.

Based on above, the self-polymerization of traditional lignin molecules into CLPs is triggered by the solvent environment, with the surface functional groups playing a pivotal role in influencing the surface wettability of these particles. Despite these studies, inconsistent or insufficient properties of the structurally heterogeneous lignin's compared to synthetic surfactants have obstructed commercialization. Consequently, aggregation of lignin in composites and phase separation in blends are common hurdles, especially with non-polar systems. To overcome this limitation, chemical functionalization of lignin by grafting polymer chains has classically been conducted. Consequently, the ongoing exploration of surface

modification techniques for lignin, with a specific focus on adjusting the hydrophilicity and hydrophobicity of functional groups, has garnered significant attention. Furthermore, as the self-assembly progresses, the gradual homogenization of surface wettability in lignin particles becomes a key factor influencing the changing driving forces for self-assembly. This dynamic process directly governs the final state of CLPs, a critical aspect closely tied to their stability at the oil–water interface. This stability, in turn, is intricately linked to the particle size and morphology, forming a complex interplay in the overall behavior and applicability of CLPs in various fields.

3.2. Surface properties of CLPs

Chemical modification of lignin is sometimes necessary to facilitate the formation of nanoparticles due to its ability to enhance the hydrophobicity of the initial lignin material, thereby resulting in a more homogeneous particle size distribution. Surface engineering plays a crucial role in modifying CLPs by recognizing the pivotal influence of the self-assembly process on their growth and distribution. The inherent stochasticity in this process presents challenges for controlling the surface wettability of CLPs, thereby necessitating the implementation of surface engineering strategies. Chemical modifications, such as amination,[102] carboxymethylation,[103] grafting,[85,104,105] or condensation polymerization of lignin surface functional groups,[88,106] provide precise approaches to reprocess and regulate surface wettability.[107,108] As demonstrated in Fig. 8, these strategies are designed to strike a balance in the number and distribution of amphiphilic functional groups on nanoparticle surfaces or adjust the surface charge of lignin particles,[90,109] effectively regulating their hydrophilicity. Through strategic chemical modifications, the surface characteristics of lignin can be tailored with precision, presenting a versatile approach to influencing how lignin interacts with its surroundings.[105]

The implementation of surface engineering strategies significantly enhances the independent controllability of CLPs surface properties. Pang *et al.*'s work demonstrates the versatility of this approach, obtaining six distinct types of CLPs by modifying the surface of alkali lignin with varying hydrophilic and hydrophobic properties.[110] The study reveals that alkyl-bridged lignin particles, exhibiting stronger hydrophobicity, display improved emulsification effects on less polar cyclohexane, while carboxymethylated lignin particles, with enhanced hydrophilicity, exhibit superior emulsification effects on more polar *n*-heptanol. Within general strategies, additive modifications such as alkylation, esterification, and chain grafting prove effective in enhancing the hydrophobic properties of CLPs.[105,111] Conversely, methods like sulfonation, phenolation, and amination are tailored to augment the hydrophilicity of CLPs,[83] offering a comprehensive toolkit for precise surface property adjustments.

Liu *et al.* applied the photoinitiated reversible addition–fragmentation chain transfer (RAFT) strategy to graft various monomers onto the lignin surface, resulting in the creation of amphiphilic CLPs with diverse structures.[89] The choice of the grafted monomer exerted a substantial influence on both the particle size and surface wettability of the CLPs. The study reveals a dynamic interplay between monomer chain length and chargeability. Shorter, electronegative monomers heighten the negative charge on the particle surface, while larger-volume monomers facilitate extensive aggregates and elongate hydrophilic chains on the particle surface. The proposed fundamental relationship between charge amount and chain length serves as a guiding principle with broad applicability across a spectrum of graft modification strategies.

Tang *et al.* demonstrated the general modification principle based on charge changes by modifying the surface of CLPs with chitosan (Fig. 8b). This resulted in the formation of lignin/chitosan nanoparticles (Lig/Chi NPs) with heightened hydrophobicity compared to CLPs alone, evidenced by an increase in the water contact angle from 41.2° to 89.7°. During Lig/Chi NP formation, the positively charged groups of chitosan interacted with the negatively charged groups of lignin. Consequently, chitosan coated the hydrophilic groups of lignin, distributing itself in the outermost layer of Lig/Chi NPs. The addition of cationic chitosan led to CLPs and Lig/Chi NPs with a soft chitosan shell structure, exhibiting opposite surface charges. Notably, the dispersion of Lig/Chi NPs was observed to be more stable due to their enhanced surface charges, highlighting a fundamental modification principle with broad applicability.[86,112]

During the construction of a new surface charge layer, the condensation of charged molecules has the potential to generate novel surface structures. Wang *et al.*, leveraging the properties of polyelectrolytes in aqueous environments, condensed single chain/geminin cationic surfactants onto the negatively charged surface of sodium lignosulfonate to construct CLPs with a cationic gel layer.[109] Driven by the hydrophobicity and π–π interactions between the aromatic groups of lignin, the weakly charged cationic active agent associated with the mixed aggregates of lignin anions, forming a coacervate with a nanoscale network microstructure. This interaction resulted in changes to the surface properties of the CLPs. Mika Henrikki Sipponen *et al.* proposed the adsorption of cationic lignin onto the CLPs surface to form dense CLPs with a positive surface charge. Studies have proved that cationic CLPs with increased cationic net charge exhibit superior performance in stabilizing Pickering emulsions in acidic environments compared to irregular solid lignin particles or unmodified CLPs. This modification underscores the potential to fine-tune the surface properties of CLPs by introducing heterogeneous charges, thereby influencing their hydrophobicity and stability at the oil–water interface.

In summary, the modification of CLPs through surface engineering involves refining the self-assembly process, specifically targeting lignin surface functional groups. This can be achieved through various chemical modifications to enhance control over surface wettability, supplying a more precise and effective approach to nanoparticle engineering. The impact of these surface property changes extends beyond individual modifications, influencing dynamic changes in the

driving forces during assembly and growth.[112] These alterations, particularly in surface properties, play a key role in deciding the particle size range of CLPs. Furthermore, the self-reactivity of lignin derived from various sources exhibits significant variability, which in turn influences the efficiency of surface modification processes. Consequently, during practical operations, it is advisable to select lignin with a high density of active sites—such as alkali lignin—or to pre-treat the precursor to enhance the exposure of additional active sites. In the upcoming discussion, the intricate relationship between particle size, distribution, and the behavior of CLPs at the oil–water interface will be explored in detail, shedding light on the multifaceted impact of surface engineering.

3.3. Morphology of CLPs

The geometry and morphology of the CLPs are to be considered as additional, critical parameter that affects their interaction at oil–water interface. It mainly includes the balance of the interaction energy of CLPs with different particle size and oil–water interface and the relative magnitude of interfacial area covered by the CLPs relative to their size.[64]

The particle size of CLPs can be adjusted using the anti-solvent precipitation property of lignin. Earlier research suggests that CLPs formation involves two concurrent processes: the surface orientation of hydrophilic segments and the adsorption of small polar lignin fragments. Controlling the nucleation size and growth rate in the self-assembly process is achievable by changing the initial concentration of lignin,[64] the rate of anti-solvent addition, the proportion of anti-solvent, and the system's pH value. Additionally, although CLPs exhibit similar particle size behavior in various anti-solvent systems, the nucleation mechanism was different. Chen *et al.* fabricated CLPs using the solvent exchange method.[65] During the experimental procedure, they investigated different solvents with mild solvating ability, such as GVL or THF. It was seen that lignin molecules maintained intramolecular stacking, where the intramolecular aromatic interaction of lignin fragment closely approximated (−5.59 kJ mol^{-1}) that observed in water, resulting in the formation of a spherical seed during the heterogeneous nucleation process (Fig. 9b).[65] When a highly concentrated solution of lignin was introduced into water, these nuclei form clusters. Subsequently, these clusters undergo further aggregation to give rise to CLPs by diffusion-limited cluster clustering, which aligned with classical nucleation theory.[113] As the solvation capacity increases, solvent molecules such as DMSO exert their influence by displacing the aromatic ring of lignin molecules from intramolecular accumulation. Consequently, this impedes the formation of spherical nuclei and subsequent aggregation into CLPs by lignin molecules.[65] Therefore, to achieve consistent and stable CLPs with a high yield using the solvent exchange method, it is crucial to employ a solvent capable of dissolving lignin while preserving its spherical core. Moreover, as shown in Fig. 9a, a solvent possessing weak solvation capacities would be more advantageous in facilitating the formation of CLPs characterized by smaller particle sizes.

The remarkable stability of Pickering emulsions primarily stems from the substantial interfacial energy of solid particles, which undergo nearly irreversible adsorption onto the oil–water interface. This adsorption process ensures the enduring maintenance of a stable state where oil and water are effectively mixed. The particle's adsorption capacity at the oil–water interface can be quantified by the desorption energy, denoted as ΔG (J):

$$\Delta G = \pi R^2 \gamma_{OW}(|1 \pm \cos\theta|)^2$$

where R is the particle radius in meters (m), γ_{OW} stands for the interfacial tension between oil and water (N m^{-1}), and θ is the three-phase contact angle between the solid, liquid, and gas phases (°). It's evident from the equation that both the particle size and its three-phase contact angle are crucial factors influencing the adsorption characteristics of solid particles. Notably, the square of the particle radius (R) is directly proportional to ΔG. The free energy of detachment divided by the thermal energy kT (where k is the Boltzmann constant, and T is the absolute temperature) is plotted as a function of the nanoparticle radius in Fig. 9c. The plot illustrates the separation energy of a single spherical particle concerning its size, with a contact angle of 90° and an oil–water interfacial tension of 27 m N m^{-1}. When particles exhibit favorable wetting conditions (*i.e.*, not too close to zero or 180°) and surpass a certain size threshold (approximately 10 nm), the desorption energy of each particle is several thousand kT.[114] Therefore, in comparison to ionic surfactants, once the particles absorb to the oil–water interface they can be effectively trapped there, due to the larger detachment free energy of CLPs solid particles, allowing them to construct more stable emulsions.[105,115]

According to the calculation formula of emulsion droplet size:

$$D = 4C\rho_p d_p V_d / m_p$$

In the formula: C is the particle interface coverage; ρ_p is the concentration of particles in the emulsion (kg m^{-3}); d_p is the diameter of the particles (m); V_d is the volume of the dispersed phase (m^3); m_p is the mass of the particles (kg). In emulsion systems, the size of the droplets is directly proportional to the particle size. A large number of studies have shown that the smaller the particle size of the emulsion droplets in the emulsion system, the higher its stability.[76]

Yu *et al.* introduced a nanomanufacturing technique involving electrospray to generate a range of CLPs characterized by distinct particle sizes and regular shapes.[116] Their investigation revealed that Olive O/W Pickering emulsions stabilized by various CLPs exhibited conventional system behavior: as the particle size increased, the size of the stable droplets also increased, while the stability of these droplets increased with smaller particle sizes. Similar observations were made in the research conducted by Ago *et al.*[84] Their findings strongly support the conclusion that when there is a higher concen-

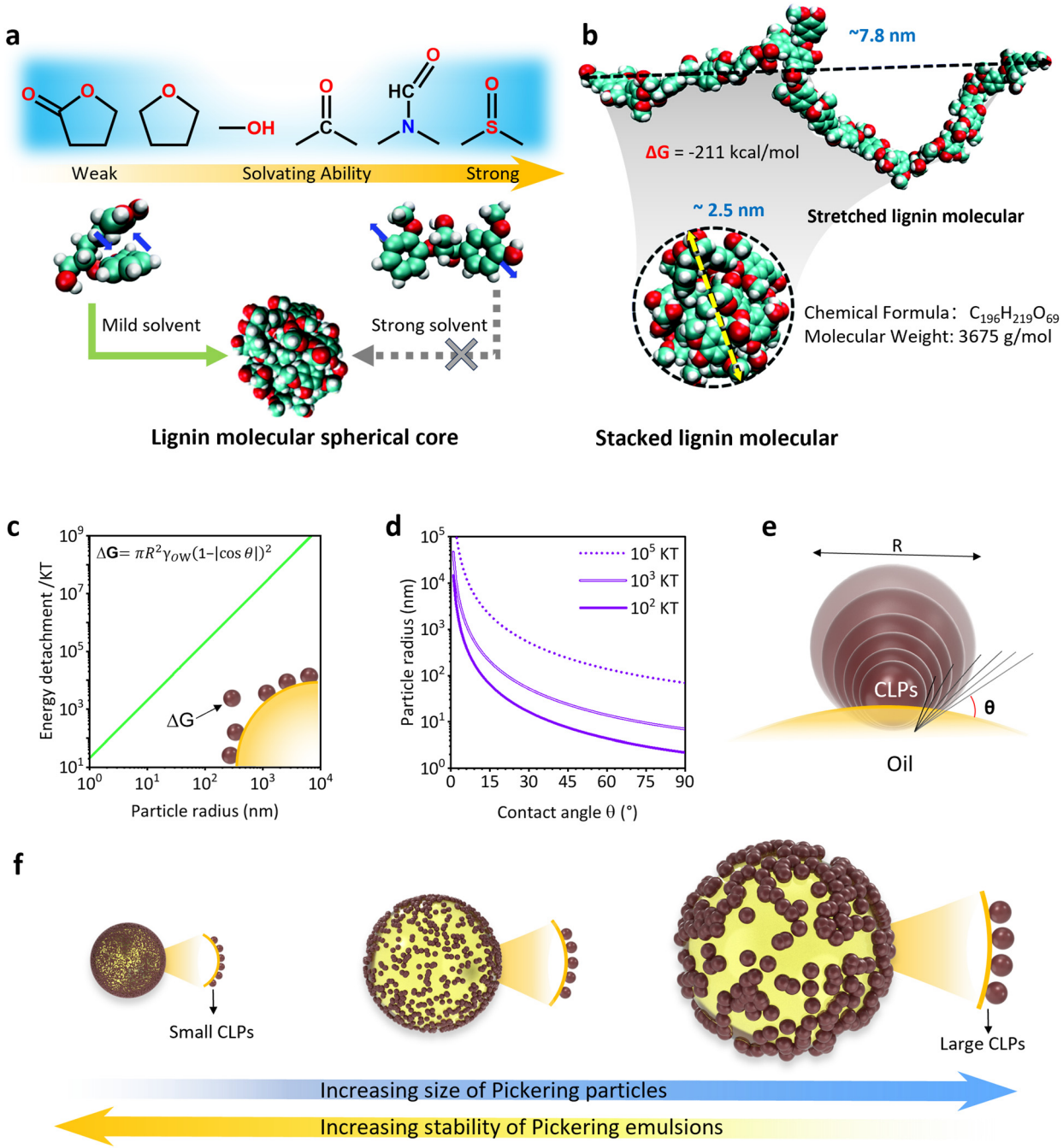

Fig. 9 (a) Formation mechanism of LNPs from different solvents.[65] Reproduced from ref. 65 with permission from Royal Society of Chemistry copyright 2022. (b) Stacked and stretched configurations of a large softwood lignin molecule.[65] Reproduced from ref. 65 with permission from Royal Society of Chemistry copyright 2022. (c) Plot illustrating the increase in energy of detachment of a single spherical particle as a function of its size (contact angle 90°, oil–water interfacial tension 27 m N m^{-1}).[114] Reproduced from ref. 114 with permission from Elsevier copyright 2014. (d) Contour plot of equal detachment energy ($\Delta G/kT$) for various particle radii and contact angles combinations.[114] Reproduced from ref. 114 with permission from Elsevier copyright 2014. (e) The contact angle of nanoparticles with different sizes at the droplet interface. (f) Different sizes of Pickering droplets stabilized by LNPs of various sizes.

tration of larger particles and smaller particle sizes, the resulting droplets tend to be smaller and exhibit improved stability.

These research findings can be summarized as follows: the size of solid CLPs has a significant impact on their flow efficiency within the continuous phase of the emulsion system and the curvature they create when adsorbed at the oil–water interface. The particle size of the emulsion droplets increases as the particle size of CLPs grows larger (Fig. 9f). This is attributed to the fact that larger particles cannot firmly adhere to the surface of smaller droplets, which have greater curvature

(see Fig. 9e). This phenomenon can be elucidated through the bending elasticity of solid particles at the oil–water interface, as described by the following formula:

$$K_s = \frac{1}{2}\sigma_{OW}\alpha^2\left(\frac{3}{4}\lambda\sin^4\theta + 5\cos^2\theta - \frac{7}{8}\right)$$

In this equation, K_s represents the surface bending elasticity of the milk droplet, σ_{OW} is the interfacial tension between oil and water, α denotes the particle radius, and λ ($\lambda = \pi/2\sqrt{3}$) is a constant. Additionally, θ signifies the particle interface contact angle. It's evident that the bending resistance of tightly packed monolayer particles at the interface is directly proportional to the square of their radius. Therefore, as the particle size of CLPs increases, the bending resistance that occurs when CLPs attach to the droplet's surface increases as well. This ultimately results in a reduction in curvature and an increase in the size of the droplet (Fig. 10a).

Moreover, the relationship between the stability characteristics of Pickering emulsions and the colloidal particle size can be understood through the Brownian motion formula:

$$D = kT/6\pi\mu\alpha$$

In this equation, D stands for the diffusion coefficient, k is the Boltzmann constant, T stands for the absolute temperature, μ is the viscosity of the liquid, and α is the radius of the particle. In comparison to larger particles, nano-sized CLPs exhibit a larger diffusion coefficient, allowing them can rapidly adsorb to the oil–water interface, facilitating the creation of smaller emulsion droplets. Subsequently, they can establish a dense physical barrier of CLPs particles on the surface of these droplets, preventing contact between droplets. However, it is not advisable to blindly optimize for small particle sizes or contact angles approaching 90° in many cases. Candidate CLPs offer more flexibility for design purposes. In Fig. 9d, contour plots depicting equal detachment energies are calculated within a specific range of particle sizes and contact angles. The enhanced stability of the Pickering emulsion can

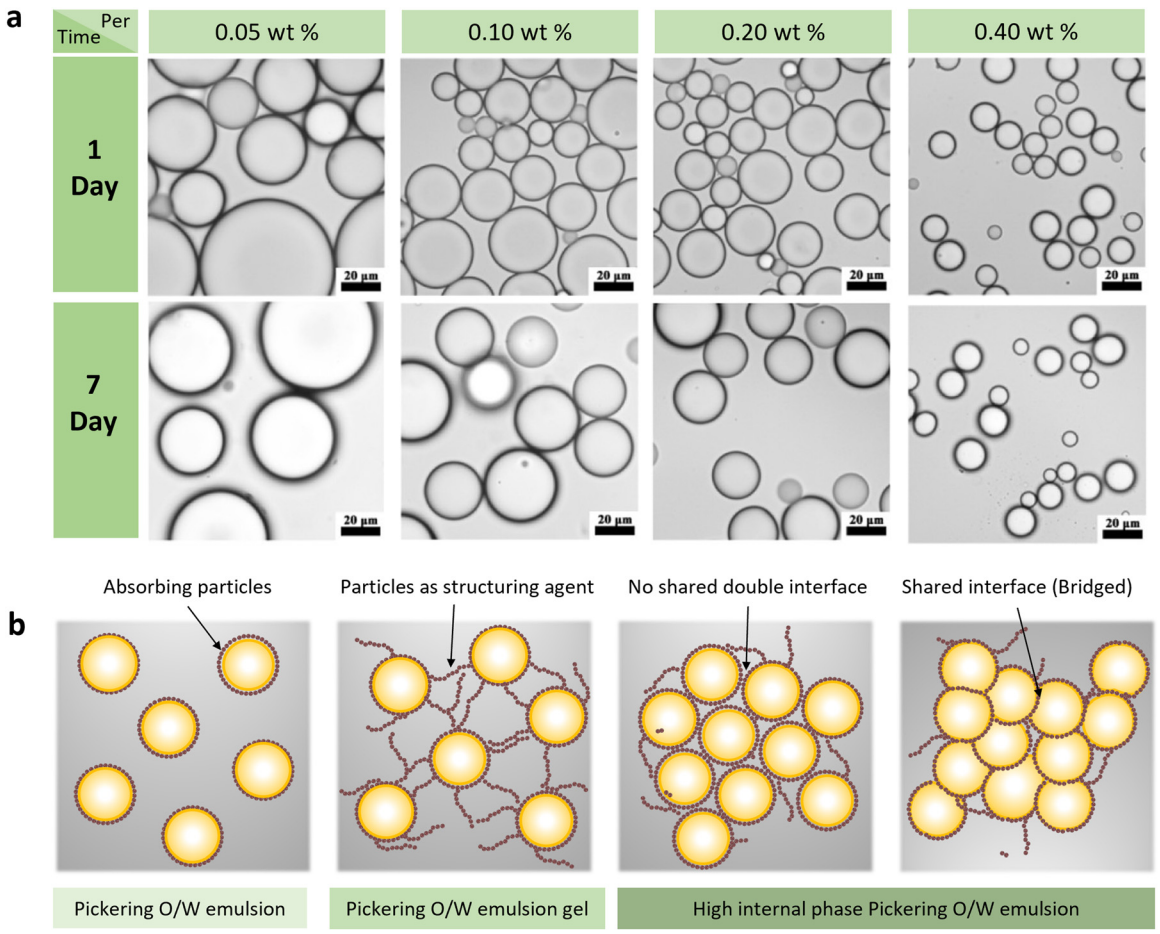

Fig. 10 (a) O.M. images of mean diameter of a lignin-stabilized Pickering emulsion using 40.0 g L^{-1}-lignin (3 : 7 v/v) with various lignin concentrations for 7 day of storage.[64] Reproduced from ref. 64 with permission from American Chemical Society copyright 2021. (b) Schematic representations of Pickering emulsions and emulsion gels incorporating particles as structuring agents in the continuous phase, along with high internal phase Pickering emulsions (HIPPEs) featuring either a single shared interface between neighboring droplets or a nonshared double interface.[127] Reproduced from ref. 127 with permission from Elsevier copyright 2020.

be attributed to the separation energy exhibited by particles at the oil–water interface, there exist various combinations of contact angles and particle sizes that fulfill this criterion.[114]

While solid particles do adsorb at the oil–water interface, they do not spread or arrange themselves in the same way surfactants do.[117] Their ability to reduce interfacial tension depends on factors like size, surface charge, wettability, and concentration, and their influence on interfacial tension is much less direct than that of surfactants.[118,119] Solid particles are much larger than surfactant molecules and cannot form a continuous monolayer at the interface. Instead of fluidly spreading across the surface to reduce tension, they lock into place, creating a mechanical barrier.[118] This makes the interfacial tension reduction a secondary or minimal effect compared to the primary stabilization mechanism (physical adsorption).[120]

3.4. Concentration of CLPs

The concentration of CLPs holds a significant sway over both particle coverage at the oil–water interface and the rheological properties of the emulsion system.[121] When the particle concentration is low in an emulsion, it fails to adequately cover the dispersed phase, resulting in flocculation and coalescence during migration, ultimately leading to the separation of the oil and water phases.

To shed light on the nuanced effects of CLPs concentration, Gordobil *et al.*[122] conducted a pivotal study systematically examining the impact of lignin concentration, oil type, and oil–water ratio on Pickering emulsion properties. Across numerous studies, a consistent conclusion emerges higher concentrations of CLPs tend to produce emulsion droplets of uniform size and stable dispersion. This conclusion gains additional support from Li *et al.*,[64] who used CLPs of varying particle sizes to stabilize Pickering emulsions of thyme oil in water. Notably, despite different CLPs sizes, all three emulsions exhibited a similar average droplet size. Significantly, the study revealed a negative correlation between the amount of lignin loaded on the oil–water interface and the particle size of the emulsion droplets-higher particle count resulted in smaller droplet sizes and improved storage stability (Fig. 10a).

Elevated lignin concentration not only influences particle interactions but also plays a crucial role in promoting increased interactions at the droplet interface. This phenomenon is driven by the presence of aromatic hydrophobic and hydrophilic fragments, inducing self-aggregation and self-organization of lignin at the interface layers. Consequently, a robust solid-like film forms around the oil droplets, effectively inhibiting flocculation, and coalescence of the dispersed phase, thereby enhancing emulsion stability.[123] As particle concentration increases, there is a corresponding rise in coverage at the oil–water interface, leading to the formation of an interface film with a specific thickness. This film plays a crucial role in inhibiting the flocculation and coalescence of the dispersed phase, ultimately enhancing the overall stability of the emulsion.[73] With continued concentration increases, particles accumulate in the continuous phase, resulting in the development of a dense bridging particle layer and a three-dimensional mesh particle layer.

These structural formations typically involve some degree of particle aggregation or droplet flocculation. Such as, in a single dense bridged particle layer, each particle, though still in the water continuous phase, becomes partially wetted by two dispersed phases and binds with adjacent particles due to attractive forces. This process leads to an elevated viscosity of the emulsion system, obstructing the migration of the dispersed phase, and consequently, reinforcing the stability of the emulsion. In high internal phase emulsion systems (volume fraction >0.74),[124] a minimal quantity of particle emulsifier is adequate to stabilize elevated concentrations of oil droplets, owing to the combined effect of adsorbed particles forming a protective layer and an aggregation network between particle-coated droplets in small gaps.[125,126] Fig. 10b illustrates two stable models for particle-stabilized high internal phase emulsions: one with continuous Pickering-stable monolayers formed by particles around each dispersed droplet, and another where multiple adsorbed particles are shared among adjacent droplets in a single-particle bridging structure. Notably, these two idealized structural arrangements often coexist in real HIPPEs systems.

This intricate interplay between particle concentration, interface film formation, and structural developments underscores the multifaceted mechanisms influencing the stability of emulsions.[128] These combined factors further reinforce the stability of the emulsion, creating a comprehensive understanding of how CLPs concentration intricately shapes the properties of Pickering emulsions.

In addition to the decisive influence brought by colloidal particles, the stability of Pickering emulsions is also affected by several factors. Factors such as the size of colloidal particles, interaction between colloidal particles, interface structure, interfacial rheology of Pickering emulsion, oil/water phase volume ratio, energy input, and emulsification process play crucial roles. These factors are interconnected and complementary, for instance, changing the pH value of the system may alter the salt ion strength, and the strong mutual attraction between colloidal particles can lead to flocculation, impacting particle size and emulsion stability. From a fundamental research perspective, plant-based materials still present various challenges in terms of optimization of functionality through the manipulation of particle size, wettability, shape anisotropy, aggregation and surface chemistry. Understanding at a greater depth how to control these factors will surely keep experimental and theoretical colloid scientists occupied over the coming years.

4. Functional applications of CLPs-Pickering materials

The global green movement has promoted widespread research and application of bio-based emulsions. The chemical composition of the lignin, as well as its size, shape, surface charge, and hydrophobicity, determine its potential application in Pickering emulsions. Many properties of lignin, such as resistance to decay and biological attack, ultraviolet absorption, high hardness,[129,130] and the ability to delay and inhibit

oxidation reactions, have enhanced its application value in composite materials. Therefore, the introduction of lignin nanoparticles into Pickering emulsions and composites based on Pickering emulsions template method can improve the properties of the materials and provide new special effects to enhance their application value.[114,131] In this section, the application fields, production methods and properties of lignin Pickering emulsions are reviewed (Scheme 3).

4.1. Application of CLPs as reinforcement in Pickering emulsions

A significant emphasis is often placed on the mechanical properties of composites. By employing rational design, diverse interactions between CLPs and matrix materials can be established, encompassing covalent bonds, hydrogen bonds, or ionic bonds (Fig. 11).[78] The incorporation of CLPs as reinforcing agents in polymer matrices and nanocomposite materials enhances crucial mechanical properties such as rigidity, strength, toughness, along with thermal stability and barrier properties of the composites for their intended applications.[74,86,132] The even dispersion of nanoparticles within a matrix poses a significant challenge for their use as reinforcing materials. The utilization of the Pickering emulsion system has gained popularity in preparing composite materials due to its ability to achieve uniform distribution of nanoparticles within the composite phase.

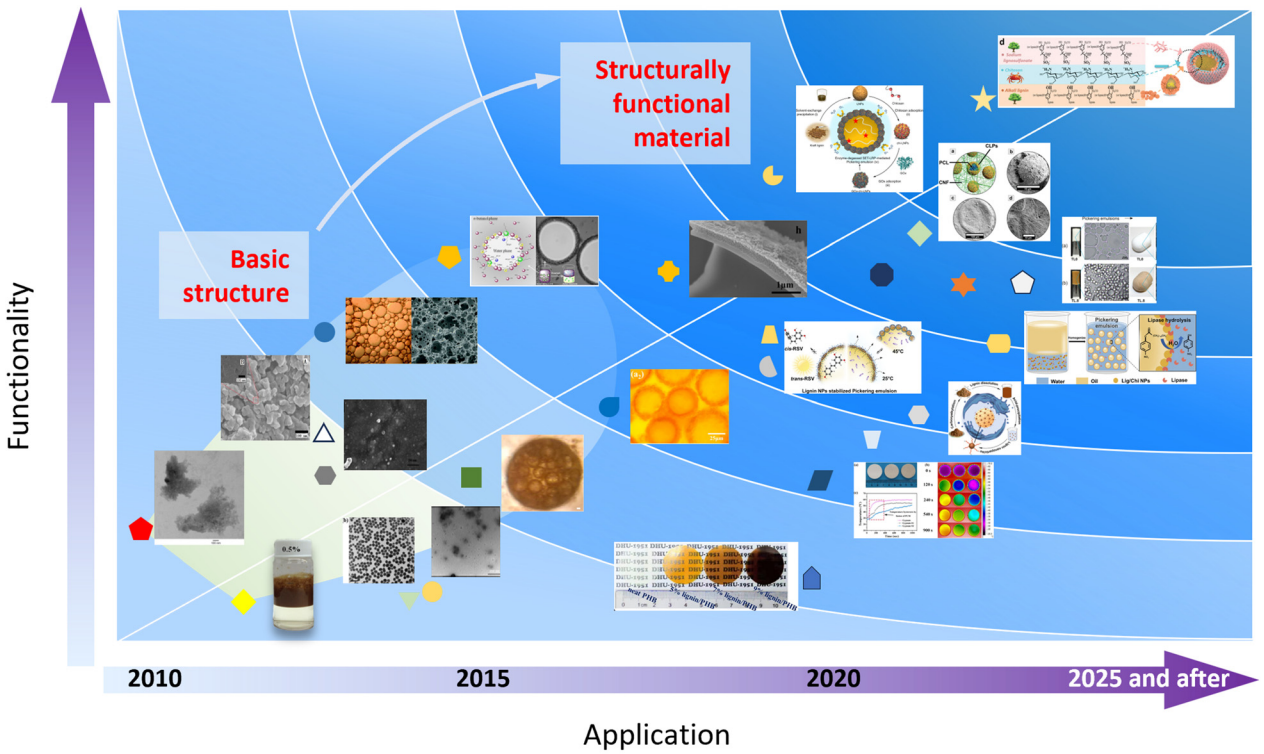

ChemPhysChem 2012, 13, 4235 – 4243
Green Chem., 2012, 14, 3230–3236
Chem. Commun.,2013, 49, 7144
ChemSusChem 2014, 7, 3513 – 3520
Chemical Engineering Journal 257 (2014) 317–327
Ultrasonics Sonochemistry 23 (2015) 369–375
Ind. Eng. Chem. Res. 2015, 54, 11501–11510
Chemical Engineering Journal 266 (2015) 299–308
Journal of Experimental Nanoscience, 11:4, 289-302
J. Agric. Food Chem. 2017, 65, 50, 11011–11019
Reactive and Functional Polymers 123 (2018) 115–121
ACS Sustainable Chem. Eng. 2019, 7, 13497–13504
International Journal of Biological Macromolecules 165 (2020) 3078–3087
Nat Commun 11, 5599 (2020)
International Journal of Biological Macromolecules 146 (2020) 1–8
Langmuir 2021, 37, 11, 3346–3358
ACS Sustainable Chem. Eng. 2021, 9, 5470–5480
ACS Sustainable Chem. Eng. 2022, 10, 29, 9334–9344
Adv. Mater. Interfaces 2022, 9, 2200988
ACS Sustainable Chem. Eng. 2022, 10, 50, 16563–16577
Langmuir 2022, 38, 42, 12849–12858
Cellulose (2023) 30:8955–8971
Chemical Engineering Journal 475 (2023) 146372
Adv. Funct. Mater. 2023, 33, 2214911

Scheme 3 The functional application development of CLPs-Pickering emulsion from 2010 to the present.

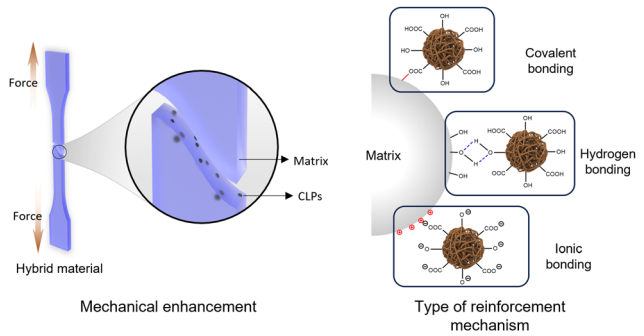

Fig. 11 Schematic illustration of lignin reinforcement and the underlying mechanisms for enhancing lignin augmentation.

In the study of Lugoloobi *et al.*,[132] the CLPs were dispersed homogeneously in the poly(3-hydroxybutyrate) (PHB) matrix to form an improved PHB composite film by employing W/O Pickering emulsion template method. Due to the uniform dispersion of CLPs and the strong interfacial adhesion between filler and matrix formed by hydrogen bond, the tensile strength and Young's modulus of the composite film increased by 13.2% and 43.9% respectively when the addition of CLPs was 7%. Li *et al.* introduced CLPs into polylactic acid in Pickering emulsion and prepared lignin/polylactic acid composite films by compression molding method.[133] The results showed that the introduction of CLPs improved the crystallinity and thermal stability of the polymer (the decomposition temperature was also increased by 10 °C). Due to the rigid structure of lignin, the Young's modulus of the composite is increased, but the pull-up property and elongation at break are decreased. This study suggests that the enhancement of CLPs depends on the properties of the substrate. It is smaller in stiff and larger in soft matrices because of the different relative load capacity of the components. Given the inherent rigidity of CLPs as a nanoparticle, in numerous studies on reinforcement, the mechanical properties of composite materials have been comprehensively enhanced through synergistic reinforcement involving multiple nanoparticles or surface grafting of CLPs.

Moreno *et al.* employed chitosan (Chi) and glucose oxidase (GOx) for surface modification of lignin nanoparticle (Fig. 12b), resulting in the synthesis of polymerized latex dispersion through free radical polymerization within a Pickering emulsion system stabilized by hybrid lignin.[88] Subsequently, nanocomposites comprising polystyrene (PS) and polybutyl methylbenenoate (PBMA) embedded with lignin nanoparticles (PS/PBMA–GOx–Chi–CLPs) were prepared *via* a melting process. The incorporation of modified CLPs significantly enhances the tensile properties of the polymer nanocomposites compared to pure PS and PBMA, without compromising elasticity. Moreover, composites reinforced with 15% hybrid nanoparticles exhibit an increase in toughness by factors of 2.5 and 15 respectively.

Similarly, the inherent properties of cellulose, lignin, and polycaprolactone were harnessed by Kimiaei *et al.* to propose a Pickering emulsion approach for the production of multifunctional CLPs hybird cellulose nanofibril (CNF) composite.[129] An aqueous dispersion of CNF was combined with hydrophobic polycaprolactone (PCL), utilizing CLPs as the emulsion stabilizer (Fig. 12a). Fabrication of CNF–PCL nanocomposite resulted in over a 134% increase in dry strength compared to nanocomposites without CLPs. The mechanism underlying the excellent dry and wet strength as well as water resistance achieved was investigated, suggesting that it is attributed to the amphiphilic nature of CLPs which can form non-covalent bonds with both cellulose and PCL, effectively binding them together.

Although CLPs can serve as nano-fillers to enhance the mechanical properties of polymers, the focus lies in improving specific tensile properties of matrix polymers, such as tensile strength, modulus, and elongation at break. It should be noted that CLPs cannot universally enhance all mechanical properties within any given matrix; rather, this synergistic effect is more likely to occur when there is good compatibility between the particles and the matrix.[18,134] Merely controlling the concentration and relative content of CLPs in composite materials often fails to achieve optimal performance improvement.[135] Therefore, surface modification strategies or collaborative enhancement involving multiple nanomaterials have been extensively emphasized with a primary objective of establishing various types of forces within copolymers including covalent bonds and hydrogen bond systems (Fig. 12c).[19,123,136] These efforts aim to construct multiple network structures capable of meeting the strengthening and toughening requirements dictated by the target application.

4.2. Application of CLPs as antioxidant in Pickering emulsions

Lignin, in its natural state, is rich in methoxy aromatic ring groups, phenolic hydroxyl groups, aliphatic hydroxyl groups, carboxyl groups and carbonyl groups, and is a natural antioxidant.[137] As demonstrated in Fig. 13a, these functional groups stop the oxidation reaction by reacting with hydrogen.[138,139] In addition, studies involving lignin nanoparticles have shown that when lignin is converted to nanoparticles, its antioxidant activity increases. This can be explained by the fact that nano-sized lignin particles have a higher surface area to volume ratio, which brings more surface antioxidant active functional sites. However, the extraction method and preparation process of lignin significantly impact the antioxidant capacity of its nanoparticles.[67] This can be attributed to variations in surface functional groups resulting from different sources of lignin raw materials and nanoparticle preparation techniques. Table 2 provides a summary of the antioxidant capacity exhibited by various lignin model compounds. Interestingly, due to the amphiphilic nature of CLPs, the antioxidant activity of the Pickering emulsion template can be directly applied to pharmaceutical, cosmetic and food processing applications.[104]

Zhang *et al.* reported a simple green method for the preparation of CLPs by water droplet induced self-assembly using deep eutectic solvent and the preparation of lignin-based

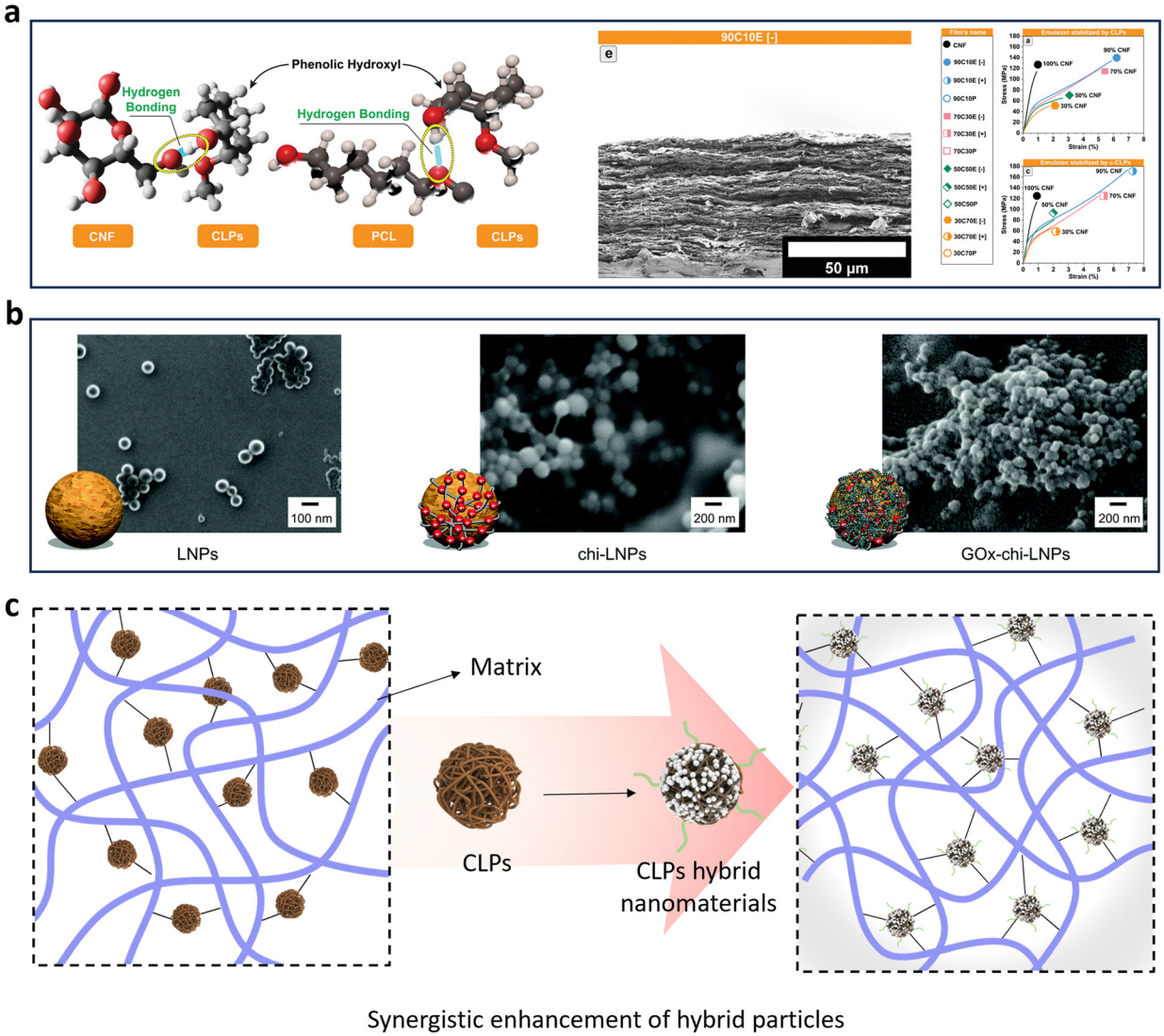

Fig. 12 (a) Schematic illustration of possible interactions between nanocomposite's components, SEM image from cross-section view and mechanical and morphological properties of neat CNF and nanocomposite films in dry condition.[129] Reproduced from ref. 129 with permission from John Wiley and Sons copyright 2022. (b) SEM images of LNPs, the adsorption of chitosan onto LNPs and GOx–Chi–LNPs produced by the deposition of GOx onto Chi–LNPs.[88] Reproduced from ref. 88 with permission from Royal Society of Chemistry copyright 2022. (c) Reinforcement mechanism of lignin hybrid particles.

Pickering emulsions with antioxidant activity.[33] They studied and compared the antioxidant activities of native lignin and CLPs based on the elimination of the π-radical (DPPH•). Fig. 13b illustrated the possible elimination reaction process of DPPH• radical by lignin. The results showed that the antioxidant activities of both samples increased with the increased of the concentration. Thanks to the increase of phenolic hydroxyl group and alcohol hidden inside CLPs, it showed higher free radical scavenging ability (up to 10%) at high concentrations (Fig. 13c). Similarly, in the study of Moreno *et al.*,[88] they evaluated the antioxidant activity of composite membranes after the combination of chitosan and glucose oxidase hybrid CLPs with PRMA through ABTS+• free radical scavenging experiments. The results showed that the antioxidant activity of PBMA supplemented with 2.5% and 5% GOx–Chi–CLPs was 30% and 70%, respectively, compared with pure PBMA (18%). However, when the content of hybrid CLPs in the composite film exceeded the concentration threshold of 10%, its antioxidant activity did not increase significantly (Fig. 13d). This result may be related to the layer-by-layer particle deposition of CLPs at the internal interface of the non-wettable polymer matrix, since the antioxidant activity is postulated to occur primarily at the liquid–solid interface. Yu *et al.* employed an electrospray technique to synthesize lignin nanoparticles with uniform size and regular shape, which were utilized for the stabilization of oil-in-water Pickering emulsions.[116] The antioxidant capacity of the Pickering emulsion was assessed by evaluating its free radical scavenging activity against ABTS and DPPH radicals. The results were quantified in terms of the concentration required to inhibit 50% of free radicals (IC50

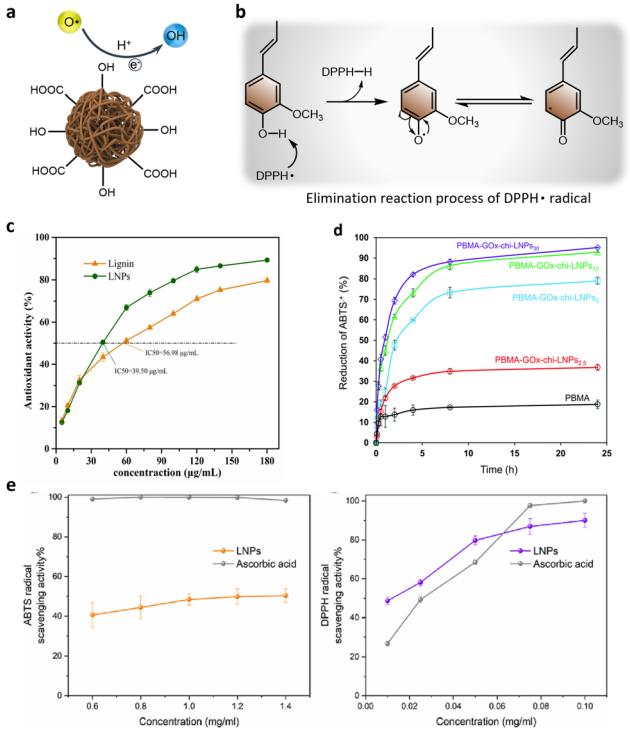

Fig. 13 (a) Schematic diagram of antioxidant mechanism of CLPs. (b) The elimination reaction process of DPPH• radical by lignin. (c) DPPH• radical scavenging activity test against lignin and LNPs.[33] Reproduced from ref. 33 with permission from Elsevier copyright 2022. (d) Antioxidant activity kinetics of pure PBMA and PBMA–GOx–Chi–LNP composite films.[88] Reproduced from ref. 88 with permission from John Wiley and Sons copyright 2021. (e) ABTS and DPPH free radical scavenging activity (%) of LNPs, ascorbic acid was used as positive control.[116] Reproduced from ref. 116 with permission from Elsevier copyright 2023.

value). Fig. 13e illustrates the investigation on the antioxidant activity of these lignin nanoparticles, revealing IC50 values of 1.3 mg ml^{-1} for ABTS quenching and 0.018 mg ml^{-1} for DPPH activity.

The study revealed that the presence of a substantial quantity of phenolic hydroxyl radicals is essential, and the abundance of methoxyl groups in lignin can stabilize the formation of phenolic hydroxyl radicals. The scavenging activity against free radicals relies on the rate at which these radicals capture hydrogen atoms from phenol molecules.[138,139] These functional groups play a crucial role in providing hydrogen to terminate oxidative propagation reactions, with free phenolic hydroxyls being indispensable for antioxidant activity.[140]

In summary, the antioxidant activity of CLPs, as a green natural antioxidant, can be directly extended to various fields including pharmaceuticals, cosmetics, and food processing by utilizing the Pickering emulsion template.

4.3. Application of CLPs as anti-ultraviolet in Pickering emulsions

Unsaturated double bonds in the molecular structure of lignin (such as carbonyl and vinyl groups) can form conjugated structures with benzene rings. Active π electrons and chromophores (such as hydroxyl, amino, ether bonds, and carboxyl groups) in conjugated systems give lignin bandwidth absorption from ultraviolet to visible light.[141] Although the various extraction processes of lignin result in different chemical structures, the ultraviolet (UV) absorption of lignin is generally similar.[142,143] The UV shielding performance of three lignin groups is illustrated in Fig. 14a. The S phenolic group containing more methoxyl groups has a stronger UV shielding property over other phenolic groups.[144,145] Because CLPs has a larger specific surface area than the original lignin at the same mass, more functional groups are distributed on the surface of the

Table 2 Summary of radical scavenging efficacy of lignin-related compounds

Compound	Number[a] of reduced DPPH
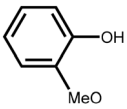	1.3
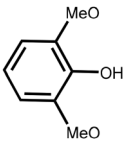	1.8
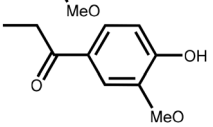	<0.1
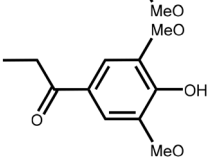	0.2
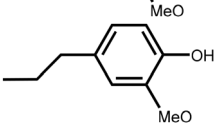	1.75
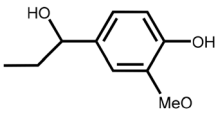	1.5
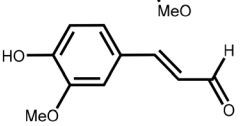	2.1
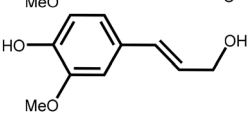	0.97
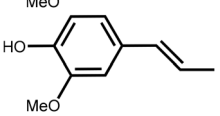	1
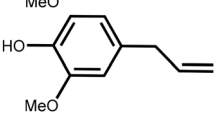	2

[a] The number of 1,1-diphenyl-2-picrylhydrazyl moles reduced by one mole of a lignin related compound.

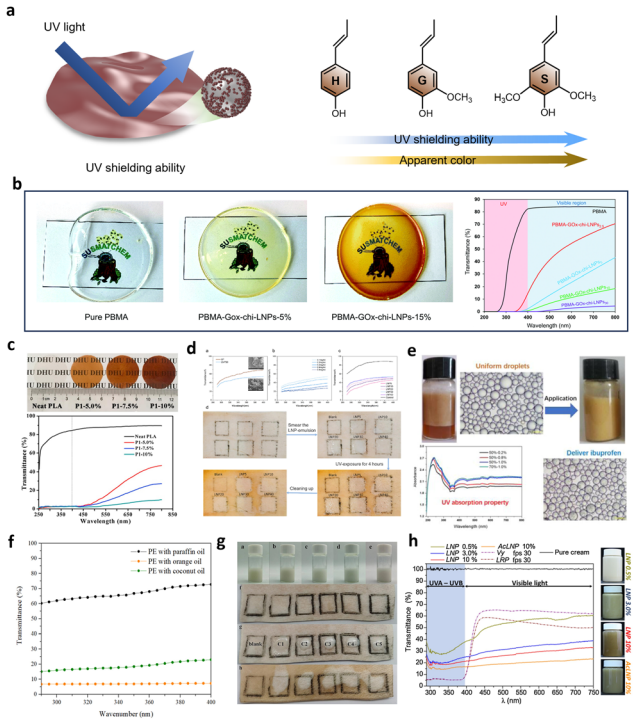

Fig. 14 (a) Schematic diagram of anti-ultraviolet properties of lignin composites and comparison of anti-oxidation properties of each unit. (b) Digital images and UV-vis light transmittance spectra of pure PBMA and PBMA–GOx–Chi–CLP composite films.[88] Reproduced from ref. 88 with permission from John Wiley and Sons copyright 2021. (c) Photographs of thin films as a function of lignin concentration (up) and UV–Vis transmission spectra of these films (down).[132] Reproduced from ref. 132 with permission from Elsevier copyright 2020. (d) UV transmittance of Pickering emulsions stabilized by CLPs and schematic illustration of pig skin to simulate human skin under strong UV-light.[116] Reproduced from ref. 116 with permission from Elsevier copyright 2023. (e) Photograph of Pickering emulsions and UV absorption spectra of the Pickering emulsion with CLPs as the stabilizer.[106] Reproduced from ref. 106 with permission from American Chemical Society copyright 2022. (f) UV transmittance of Pickering emulsions prepared with 3.50 wt% of CLPs and 40% of oil.[122] Reproduced from ref. 122 with permission from Elsevier copyright 2023. (g) Schematic illustration of pig skin to simulate human skin under strong UV-light.[142] Reproduced from ref. 142 with permission from Springer Nature copyright 2024. (h) UV-vis transmittance curves and appearance color of creams with different amounts of CLPs.[146] Reproduced from ref. 145 with permission from Elsevier copyright 2020.

lignin particles, which has better UV resistance. In addition, the improved performance depends on the effective interfacial adhesion and uniform dispersion of CLPs within the polymer body, which is a problem that cannot be ignored, and Pickering emulsions not only avoid the agglomeration problem of CLPs, but also allow their introduction into the hydrophobic polymer.

Moreno *et al.* evaluated the UV shielding potential of PBMA–GOx–Chi–CLPs composite films prepared by them by using UV-Vis colorimetric spectroscopy.[88] The results show that the composite films have strong absorption in UV-A (315–400 nm) and UV-B (280–315 nm) bands compared with the original PBMA. They also highlight that even a concentration of only 5 wt% of GOx–Chi–CLPs in the composite can reduce UV light transmission to 3% with a reduction of only 40% in visible light transmission (Fig. 14b). In the study of Lugoloobi *et al.* CLP–PHB composite films with yellowish brown color and good UV isolation performance were prepared by using Pickering emulsion method.[132] With the increase of the proportion of CLPs in the composite film, the UV shielding performance of the film is gradually enhanced, and the light transmittance is gradually decreased (Fig. 14c). This is not only due to the increased absorption of ultraviolet and visible light by more CLPs, but also due to the increased reflection and refraction of incident light by high content of nanoparticles. A similar conclusion was also reached in a study by Li *et al.*[133]

Yu *et al.* found that lignin nanoparticles with smaller particle size had better anti-ultraviolet performance.[116] In addition, they emphasized that the methoxyl functional groups in S-type and G-type lignin, which were easy to absorb UV light, could also significantly promote the conjugated system of lignin, and thus have stronger UV absorption (Fig. 14d).[145] Hong used sulfur methylation and alkyl chain bridging modification of lignin to prepare Pickering emulsions. As shown in Fig. 14e, the introduction of higher molecular weight alkyl chains effectively enhanced the stability of the emulsion, allowing it to maintain strong UV absorption capacity even at low lignin loading (0.2%) and oil–water ratio (50%).[106]

Cosmetics with natural light protection properties are an ideal application direction for lignin's anti-UV performance.[143] The CLPs were prepared by Gordobil *et al.* using softwood sulfate lignin as the raw material, and three O/W Pickering emulsion systems of orange oil, coconut oil, and paraffin oil were formulated.[122] In vitro sun protection factor (SPF) testing demonstrated that these Pickering emulsions exhibited UVA/UVB values ranging from 0.74 to 0.90 with $C > 380$, confirming their broad-spectrum sunscreen efficacy. Furthermore, the incorporation of natural oils containing phenolic compounds into the emulsion system enhanced its SPF value (Fig. 14f), whereas paraffin oils did not show such improvement due to the synergistic effect of π–π stacking between lignin particles and phenolic compounds. The CLPs were extracted from coffee beans through acid precipitation by Xin *et al.*[142] Subsequently, the obtained coffee CLPs was utilized to formulate a stable Pickering emulsion, which underwent UV resistance testing. Notably, the results demonstrated that even after 4 hours of exposure to 254 and 365 nm UV light, the emulsion effectively preserved pigskin color (Fig. 14g). Trevisan *et al.* isolated nano-lignin from elephant leaf grass, which can be stably dispersed in commercial neutral creams and significantly improve its UV-visible shielding properties.[146] Although the general fact is that the higher the concentration of lignin, the stronger the protection against UV rays. However, the undesirable dark color appearance of CLPs based sunscreen creams and composite and will be its limitations in some applications, such as cosmetics (Fig. 14h). Thus, light-colored lignin with

anti-ultraviolet activity is important, which can be achieved through the acetylation of the lignin and subsequent conversion into nanoparticles. In addition, the improved performance depends on the effective interfacial adhesion and uniform dispersion of CLPs within the polymer body, which is a problem that cannot be ignored, and Pickering emulsions not only avoid the agglomeration problem of CLPs, but also allow their introduction into the hydrophobic polymer. In addition, the UV-resistant properties of lignin particles can also be used for protection against photosensitive drugs, which will be discussed in the next section.[104,147,148]

4.4. Application of CLPs as encapsulation in Pickering emulsions

Contributed to its amphiphilicity and good biocompatibility, lignin is considered as a promising drug delivery material.[149] In the Pickering emulsion system, CLPs can be used to achieve the loading and controlled release of various drug molecules, such as drug activity, sunscreen activity, model drugs, agricultural chemicals and even enzymes,[80,86,109,147,148,150] through embedding and encapsulation. Based on the characteristics of CLPs, the use of CLPs for drug encapsulation has the following obvious advantages: 1. Protect sensitive chemicals from decomposition, evaporation and degradation caused by external environmental factors.[104] 2. Prolonging the duration of the drug effect by controlled release;[85] 3. Reduce the toxicity and stimulation of the drug to non-targeted organisms.[151]

According to the type of encapsulated drug and application field, two different encapsulation ideas are proposed (Fig. 15). One is to prepare solid CLPs and use Pickering template method to achieve encapsulation of photosensitive drugs.[109] The other is to use interfacial emulsion polymerization method to prepare lignin microcapsules and realize the encapsulation of drugs through cross-linking reaction in microemulsion system.

For example, Wang *et al*. used single-chain/gemini surfactants and sodium lignosulfonate to prepare water-based agglutinates for stabilizing O/W emulsions.[109] Attributed to the nanoscale network structure of a wide range of hydrophilic and hydrophobic microdomains in the condensate (Fig. 16a), it can achieve encapsulation and anti-ultraviolet protection against photosensitive pesticides (photosensitive abscisic acid). Chen *et al*. prepared an O/W high internal phase emulsions (HIPEs) with an internal phase fraction of up to 80 vol% using 5 wt% lignin and 1 wt% sodium dodecyl sulfate (SDS) as emulsifiers.[148] The photosensitive bio-anti-inflammatory agent curcumin was dispersed in the organic phase and effectively encapsulated in HIPEs. As shown in Fig. 16b, the CLPs aggregation on the surface of HIPEs could be adjusted by using PBS buffer to control the release of the reagent. As shown in Fig. 16b down, after 72 hours of ultraviolet irradiation, curcumin encapsulated with 3 wt% CLPs-stabilized HIPEs was able to maintain 60.3% of its original concentration.

Due to the differences in drug electronegativity, release speed, release environment and efficacy mechanism, encapsulation materials with corresponding different stimuli have been widely emphasized.[80,85,104,154,155] Consequently, stricter requirements are placed on the charge properties, wall thickness, polydispersity, and stability of CLPs as carriers for drug transport.[26,31] To address this need, researchers have developed a series of packaging systems that exhibit both stability and environmentally induced response through hybrid modification of lignin or layer assembly.[83,102,106,112]

Dai *et al*. grafted poly(*N*-isopropylacrylamide) (PNIPAM) onto lignin to prepare thermoresponsive lignin copolymers.[104] The hybrid CLPs were formed by self-assembly to stabilize *trans*-resveratrol (*trans*-RSV)-containing palm oil emulsion droplets in water. Contributed to the excellent UV resistance of lignin, *t* the light stability of *trans*-RSV was significantly improved by the protecting of the CLPs layer. Moreover, the emulsion properties and release behavior strongly depend on the temperature and nanoparticles size: decreasing temperature induced deformation of hybrid CLPs at the interface, an increase in droplet size, and the accelerated release of *trans*-

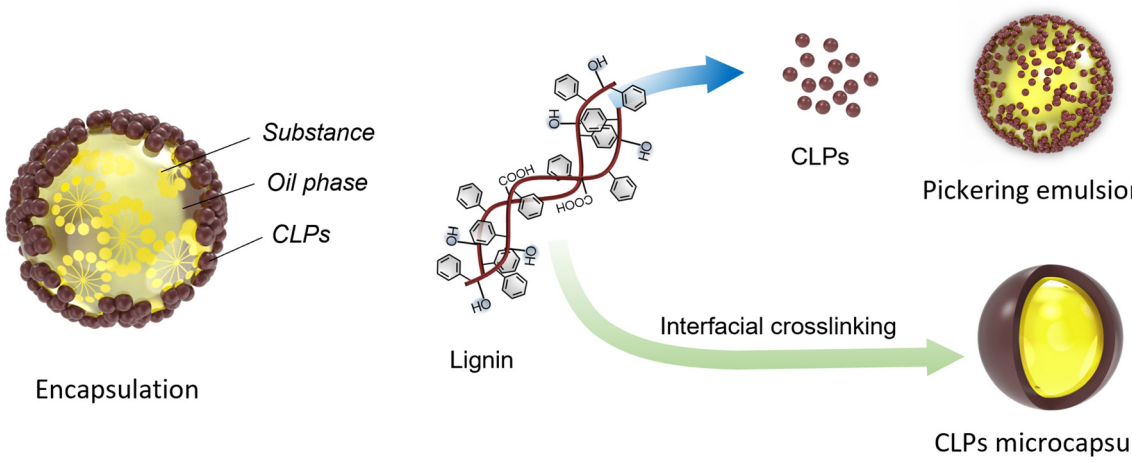

Fig. 15 Schematic representation of CLPs as a encapsulation material and two encapsulation processes.

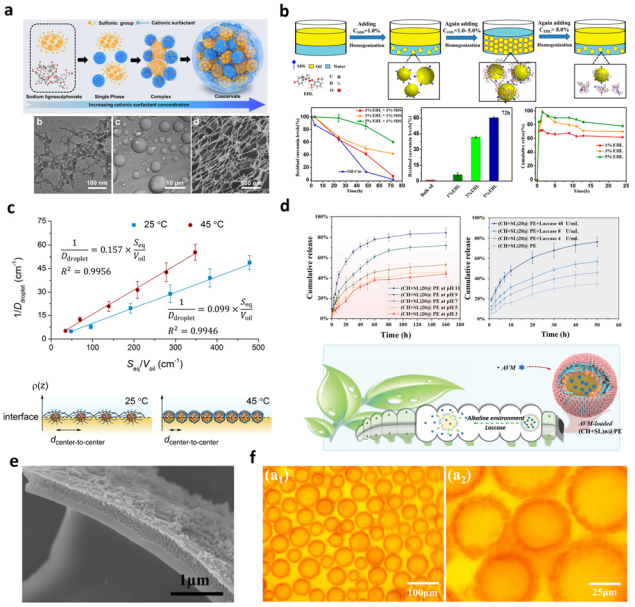

Fig. 16 (a) Formation of lignin-based coacervates and TEM image CLPs and Bright field microscopy and cryo-SEM image of coacervate droplets in mixed solution.[109] Reproduced from ref. 109 with permission from Elsevier copyright 2022. (b) Mechanism diagram of the HIPEs stabilized by CLPs and SDS (up) and residual curcumin levels in HIPEs-cur prepared with various CLPs concentrations after UV radiation and release profiles of curcumin from HIPEs stabilized with various CLPs concentrations (down).[148] Reproduced from ref. 148 with permission from American Chemical Society copyright 2018. (c) Influence of the amount of AL-*g*-PNIPAM NPs on emulsions droplet size at 25 and 45 °C (up), schematic representation of the adsorbed AL-*g*-PNIPAM NPs at 25 and 45 °C (down).[104] Reproduced from ref. 104 with permission from American Chemical Society copyright 2019. (d) Effects of pH and laccase on the release performance of AVM from (Chi + SL)20@PE Pickering emulsion and schematic diagram of pH/laccase-responsive release of AVM-loaded microcapsules (Chi + SL)*n*@PE in pests.[112] Reproduced from ref. 112 with permission from John Wiley and Sons copyright 2023. (e) SEM images of wall layer structure of lignin–polyurea shell microcapsule.[152] Reproduced from ref. 152 with permission from Elsevier copyright 2018. (f) Optical microscopy images of the lignin/polyurea composite microcapsules.[153] Reproduced from ref. 153 with permission from American Chemical Society copyright 2017.

RSV (Fig. 16c). Similar strategies have been applied in Wen *et al.*'s study.[155]

Yu *et al.* deposited chitosan (Chi) and sodium lignosulfonate (SL) alternately on the interface of CLPs-based Pickering emulsion by electrostatic interaction, formed a simple and effective Pickering emulsion strengthening strategy.[112] The prepared Pickering emulsion has adjustable interface thickness with strong stability and forms a microcarrier suitable for the coating of hydrophobic and photosensitive pesticide Avermectin (AVM). As shown in Fig. 16d, the drug release behavior of CLPs-Pickering emulsion can be carefully controlled by controlling the number of sediment layers.[86] In addition, the encapsulation system has special stimuli response behaviors for the alkaline environment and laccase stimuli in the insect digestive tract to realize the targeted release of drugs.

Pang *et al.* realized the encapsulation protection of AVM by using interfacial emulsion polymerization in lignin-stabilized O/W emulsions.[152] In this study, diphenyl methane diisocyanate (MDI) and AVM were dispersed in toluene to form an oil phase. During the preparation of Pickering emulsion, MDI in the oil phase would react with water and phenolic hydroxyl of lignin at the oil–water interface to form a thin polyurea layer and lignin–polyurethane shell (Fig. 16e). Ethylenediamine (EDA) is introduced into the system to accelerate shell formation and increase wall thickness. The study of drug release kinetics showed that controlled release of drugs could be achieved by controlling lignin content in emulsion system. Further observation of the wall layer of the formed microcapsules showed that the wall structure was composed of a dense polyurea inner layer and a loose and porous lignin–polyurethane outer layer. The increase of lignin content would consume more MDI, thus reducing the thickness of the polyurea layer and accelerating the release of drugs. Similarly, Pang *et al.* applied hybrid CLPs to a stable Pickering emulsion and prepared microcapsules containing lignin.[153] In this study, a "physical sulfonation" strategy was proposed for lignin. SDS was used to doping acidified alkaline lignin to obtain negatively charged SDS–CLPs. At the oil–water interface of Pickering emulsion, isophorone diisocyanate (IPDI) in the emulsion droplets reacts with ethylenediamine to form a strong polyuurea shell (Fig. 16f), while SDA–CLPs can crosslink with positively charged thylenediamine hydrochloride ion (EH) to form an outer gel shell, thereby improving the stability of the system and controlling the release of encapsulated drugs.

The preparation of environmentally appropriate lignin microcapsules is also the development direction of interfacial crosslinking method. Chen *et al.* synthesized pH-responsive lignin microcapsules and encapsulated coumarin-6 in a microemulsion system by heat-induced interfacial crosslinking.[85] In this study, the allyl group was grafted onto the surface of water-soluble lignosulfonate by etherification reaction, and then the oil–water microemulsion system was prepared with the help of SDS. At the oil–water interface of microemulsion system, amphiphilic lignin and the organic phase crosslinker trimethylolpropane tris(3-mercaptopro-pionate) through the free radical induced thiol–ene reaction lignin nanocapsules were formed by cross-linking. The study found that the acid-labile β-thiopropionate cross-linkages in microcapsule wall layer induced an acid-triggered quick release in low pH environment. In acidic (pH = 4) environments, the cumulative 48 hour release of coumarin-6 reached 60%, compared to 40% in neutral (pH = 7.4) environments.

In summary, the use of CLPs as a carrier for drug or chemical appears to be the most widely application, including biomedicine, agricultural chemicals and so on.[29,148,150,154] The types of encapsulated drugs involved in these applications, the use environment, the target and the release cycle, *etc.*, need to be considered as the criteria for the preparation of lignin microcapsules. The selection of the packaging process of lignin should be more differentiated from different fields, in

the field of pesticide-controlled release grade plant protection, the selection of hybrid lignin with lower purity, and in the field of biomedicine, purified or graded lignin should be considered.[34,154] In particular, the introduction of the concept of composite materials requires CLPs-based microcapsule systems to have more versatile properties, such as magnetic lignin-based Pickering emulsion and highly absorbent lignin-based gel systems.[115,156] Overall, the CLPs can serve well as an effective Pickering stabilizer for emulsion, not only due to its excellent partial wettability but also its stimuli-tunable surface properties, which allowed the facile and rapid reversible emulsification/demulsification of Pickering emulsion.[26] This poses a challenge to the researchers' knowledge background and to lignin, whose macromolecular structure is not yet fully understood. However, CLPs has been widely accepted as a green, bio-friendly, multi-functional packaging material.

4.5. Application of CLPs as catalysts in Pickering emulsions

Due to its diverse hydrophilic and hydrophobic functional groups, along with acidic and basic active sites on the surface, lignin has emerged as a catalyst with enhanced reactivity.[157,158] In numerous studies, catalysts derived from lignin have proven to be a highly promising alternative to traditional catalysts, offering advantages such as eco-friendliness, reusability, and efficiency. The use of lignin as a catalyst contributes to a greener environment by utilizing renewable sources, in contrast to conventional heavy metal catalysts like titanium and palladium, which can have detrimental effects on the environment during disposal.[159]

The various benefits of CLPs over their macro-sized counterparts suggest the potential for improved catalytic activity. In catalytic reactions, a critical parameter is the surface area, which can enhance conversion rates and ultimately improve yields. Therefore, employing CLPs with a higher surface area-to-volume ratio, in comparison to conventional lignin, holds promise for the development of novel and environmentally friendly catalysts with superior catalytic performance.

Tang *et al.* developed positively charged chitosan hybrid lignin nanoparticles (Lig/Chi NPs) for stabilizing O/W Pickering emulsions.[160] The modification with chitosan enhanced the lignin-emulsion's stability, emulsification properties, and resistance to salt and alkali. Furthermore, they investigated the catalytic impact of lipase on the hydrolysis of *p*-nitrophenol palmitate within this system. The results indicated that the Pickering emulsion system increased the interface area for significant oil–water reactions. The negatively charged lipase was effectively adsorbed onto the surface of positively charged hybrid lignin through electrostatic adsorption and enrichment, thereby reducing mass transfer distances and resistance (Fig. 17a). In this system, the reaction conversion rate can reach nearly 100% within 30 minutes, which is almost three times higher than that of the conventional two-phase system (Fig. 17b). Additionally, lipases stabilized in Pickering emulsion exhibit strong recyclability, thanks to the protective effect of Lig/Chi NPs.

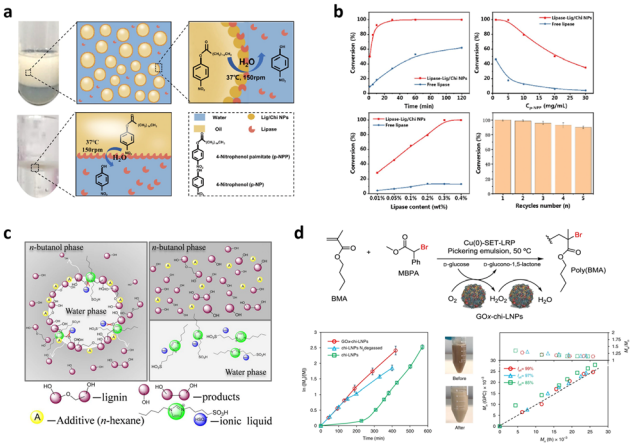

Fig. 17 (a) Schematic of lipase-catalyzed hydrolysis of *p*-NPP in the Pickering emulsion system stabilized by Lig/Chi NPs and the conventional two-phase system.[160] Reproduced from ref. 160 with permission from American Chemical Society copyright 2022. (b) The effects of reaction time, *p*-NPP concentration, lipase content and recycle times on catalytic performances of lipase in the conventional two-phase system and Pickering emulsion system stabilized by Lig/Chi NPs.[160] Reproduced from ref. 160 with permission from American Chemical Society copyright 2022. (c) Proposed emulsion reactor and W/O interface. Reproduced from ref. 162 with permission from American Chemical Society copyright 2015. (d) Evaluation of the enzyme-degassed controlled radical polymerization of BMA using GOx–Chi–LNPs as stabilizers.[161] Reproduced from ref. 161 with permission from Springer Nature copyright 2020.

In addition to using CLPs at the emulsion interface to enhance catalytic efficiency, the Pickering emulsion system can also facilitate the catalytic cracking of lignin itself. For instance, Cai *et al.* pioneered a novel and highly efficient lignin depolymerization W/O Pickering emulsion, employing lignin as a self-surfactant.[162] The Pickering emulsion was prepared using *n*-butanol and *n*-hexane as the oil phase and lignin as the emulsifier, achieved by dissolving an ionic liquid in the water phase. In the emulsion system, lignin serves a dual purpose: it not only stabilizes the emulsion but also degrades at the water–liquid interface (Fig. 17c). This results in the exposure of hydrophilic α-O-4 and β-O-4 connection points in lignin to the oil–water interface, facilitating enhanced contact with the IL catalyst and significantly promoting lignin depolymerization.[162]

Moreover, the system offers advantages in the demulsification process, with automatic phase division occurring at the end of the reaction due to lignin degradation and condensation. Following the reaction, two distinct phases emerge: the depolymerization product dissolves in the upper phase of the *n*-butanol dispersion, while the IL catalyst is present in the lower phase of the water. This enables efficient product separation and catalyst recovery through a one-step separation and filtration process. The results indicate that lignin depolymerization at the oil–water interface has a significant impact. Under optimized conditions, the conversion rate of bagasse lignin exceeded 89.1%, the selectivity of 4-ethylphenol was

53.9%, and the yield of 4-ethylphenol was 29.60 mg g^{-1} (3.3 times higher than that without emulsion).

In the study of Moreno *et al.*, they show that lignin nanoparticles (LNPs) coated with chitosan and glucose oxidase (GOx) enable efficient stabilization of Pickering emulsion and *in situ* enzymatic degassing of single electron transfer-living radical polymerization (SET-LRP) without extraneous hydrogen peroxide scavengers.[161] The feasibility of GOx–Chi–LNPs to provide an oxygen-tolerant and controlled polymerization process was evaluated by the polymerization of butyl methacrylate (BMA) as a model monomer in closed vials to avoid the loss of volatile BMA from the reaction mixture. These results (shown in Fig. 17d) not only validate our original hypothesis and confirm GOx–Chi–LNPs as efficient degassing stabilizers for Pickering emulsions polymerizations, but also demonstrate that GOx–Chi–LNPs can provide even a faster polymerization rate than Chi–LNPs after applying nitrogen purging, which could be of potential interest for industrial applications.

4.6. Application of CLPs as adsorbent in Pickering emulsions

Leveraging the structural characteristics of lignin and the functional groups present within its molecular framework, surface engineering or nanotechnology can be employed to modify its spatial network architecture. This approach facilitates the development of lignin-based adsorbent materials exhibiting superior adsorption capabilities. Such materials serve as viable alternatives to costly activated carbon and ion exchange resins for the efficient removal of heavy metal ions, dyes, and organic pollutants. In comparison to conventional lignin powders, CLPs exhibits enhanced affinity towards the oil/water interface due to its larger contact area between oil and water phases. This unique characteristic renders CLPs a promising template for the development of novel adsorbents in Pickering emulsion systems. The optimized interaction between oil and water phases within the Pickering emulsion system ensures superior adsorption performance.

In the study conducted by Padilha *et al.*, corncob (CC) and green coconut fiber (GCF) were utilized for the preparation of two CLPs.[121] The Pickering emulsion template method was employed to compare the adsorption capacity of these CLPs towards emulsified oil in a water environment. The results indicate that at an CLPs concentration of 2 g L^{-1}, CC–CLPs and GCF–CLPs exhibited maximum removal values of 90.6% and 94.4%, respectively, in emulsified oil experiments (Fig. 18a). Due to its higher lignin content, GCF–CLPs demonstrated enhanced hydrophobicity, resulting in superior ability to remove emulsified oil. This stronger hydrophobic interaction led to gradual adhesion between CLPs layers near the droplets, thereby increasing aggregate size and enhancing their oil adsorption capacity.

Agustin *et al.* harnessed the synergistic effect of nanocellulose on CLPs to achieve stabilization of polyethylene in O/W Pickering emulsion.[134] By adjusting the content of CLPs in the emulsion, the interaction with the oil phase can be finely tuned to produce a stable emulsion with varying viscosity. The resulting freeze-dried cellular foam exhibits promising potential as an adsorbent for pharmaceutical contaminants, while the incorporation of CLPs facilitates efficient removal of aromatic drugs possessing diverse ionic properties (Fig. 18b). Additionally, due to lignin's various active functional groups (such as hydroxyl, carbonyl, carboxyl, methyl), chemical modifications can be made to obtain efficient lignin-based adsorption materials. This not only enhances the commercial value of lignin but also opens up new avenues for its high-value utilization. The research conducted by Yang *et al.* demonstrates a versatile and straightforward approach for the formation of interconnected foams templated from Pickering-HIPE using a coactive system consisting of CLPs and monomers.[125] It has been observed that the foam structure transitions from closed-cell to open-cell as the concentration of monomers increases.

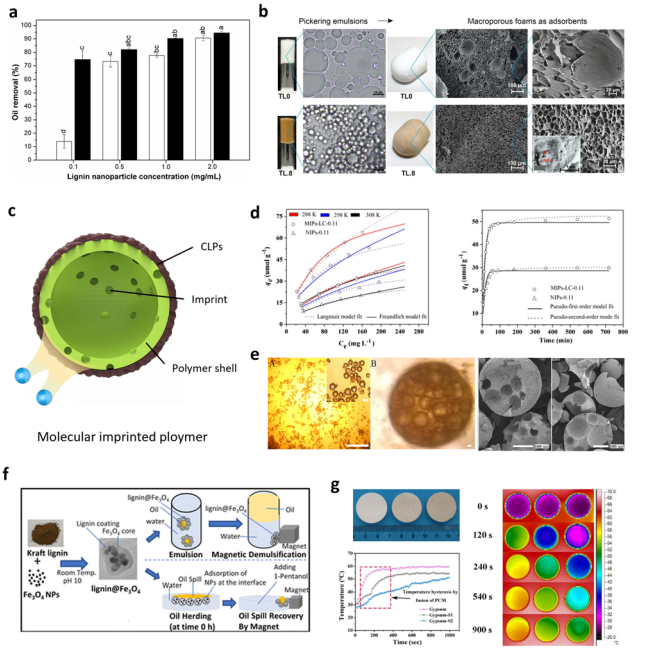

Fig. 18 (a) Effect of the CC-LNP (white bar) and GCF-LNP (black bar) for separation of emulsified oil by coagulation.[121] Reproduced from ref. 121 with permission from Elsevier copy 2020. (b) The appearance and droplet morphology of the Pickering emulsions stabilized by CLPs-CNF and the subsequent foams, with respective SEM images.[134] Reproduced from ref. 134 with permission from Springer Nature copyright 2023. (c) Schematic diagram of imprinted molecular. (d) Equilibrium data and modelling for the adsorption of LC onto MIPs-LC-0.11 and NIPs-0.11 at different temperature (left) and kinetic data and modelling for the adsorption of LC onto MIPs-LC-0.11 and NIPs-0.11(right).[163] Reproduced from ref. 163 with permission from Elsevier copyright 2014. (e) Optical microscope images of the primary W/O emulsions with W : O of 1 : 1 and the corresponding double $W_1/O/W_2$ emulsion and SEM images of multi-hollow microsphere.[164] Reproduced from ref. 164 with permission from Elsevier copyright 2015. (f) Construction strategy and mechanism of magnetic CLPs stabilized Pickering emulsion.[156] Reproduced from ref. 156 with permission from Royal Society of Chemistry copyright 2023. (g) Optical photos, infrared camera images and the surface temperature of pure gypsum and GS@TDA/PMMA/MPC. Reproduced from ref. 166 with permission from American Chemical Society copyright 2020.

Furthermore, these interconnected foams exhibit exceptional adsorption capacity for $Cu2^{+}$ ions.

In Gan *et al.*'s study,[163] CLPs were employed as stabilizers to establish a stable Pickering emulsion. By incorporating functional and cross-linked monomers along with Lambda-cyhalothrin (LC) as template molecules, into the oil phase, a molecularly imprinted polymer (MIPs-LC) was prepared *via* interfacial polymerization method for selective adsorption of LC (Fig. 18c). The surface hydrophobicity of MIPs-LC obtained after emulsion polymerization was enhanced, facilitating the adsorption of hydrophobic organic pollutants with low water solubility such as LC molecules. Preliminary results demonstrated that MIPs exhibited excellent recognition towards LC, with an adsorption equilibrium time of approximately 3.0 h and an equilibrium adsorption capacity of 72.25 lmol g^{-1} compared to nonimprinted polymers (NIPs) which showed an adsorption capacity of 43.10 lmol g^{-1}. Isothermal curve analysis, adsorption kinetics studies, and selectivity tests collectively indicated that LC had the highest cavity matching with the imprinted polymer due to its structural characteristics and hydrogen bonding interactions formed within the imprinted cavities (Fig. 18d). Furthermore, the synthesized MIPs could be effectively regenerated and recycled for at least three cycles without significant loss in their adsorption capacity (8.73%).

Similarly, Pan *et al.* conducted a facile chemical modification of lignin using oleic acid, followed by stabilizing the original and modified lignin at two interfaces to form a surfactant-free water-in-oil-in-water ($W_1/O/W_2$) Pickering double emulsion.[164] Molecular-imprinted hollow spheres (MIMMs) with adjustable pore structures were prepared by manipulating the volume ratio of the oil phase to the water phase in the emulsion and investigated as adsorbents for selective and efficient removal of LC (Fig. 18e). The static adsorption experiment revealed that MIMMs with increased and larger pore structures exhibited enhanced selective adsorption capacity towards LC. The equilibrium adsorption capacity of MIMMs for LC was determined to be 24.79 mg g^{-1}, with an adsorption equilibrium time of approximately 3.0 hours. Furthermore, MIMMs demonstrated excellent regeneration capability through seven effective regeneration and recirculation cycles, making this approach applicable for the adsorption of various pharmaceutical compounds.

4.7. Other application of CLPs in Pickering emulsions

Additionally, the potential applications of CLPs-Pickering emulsions can be further expanded through their combination with other novel technologies and materials.[165] Hasan *et al.* demonstrated the adsorption and magnetic properties of lignin@Fe_3O_4 at the castor oil–water interface as an environmentally friendly magnetically controllable Pickering emulsion and polymer oil stabilizer for oil spill collection using external permanent magnets with varying magnetic fields (Fig. 18f).[156] Wang *et al.* investigated microencapsulation using a CLPs-stabilized Pickering emulsion, which when combined with gypsum resulted in an effective heat-storage composite material that holds promising prospects for building thermal management (Fig. 18g).[166] Yi *et al.*, fabricated multilayered composite microcapsules coated with isophorone diisocyanate (IPDI) healing agent using an oil-in-water Pickering emulsion stabilized by lignin nanoparticles as a template.[91] This technology was applied to anticorrosive polymer coatings by incorporating these microcapsules into epoxy coatings. Results from salt immersion accelerated corrosion tests demonstrated that the self-healing coatings containing IPDI capsules exhibited a remarkable anticorrosive effect on steel plates. After immersing the samples in a 10% wt% NaCl solution for 120 hours, no visible signs of corrosion were observed on the coating matrix due to the controlled release and subsequent polymerization of active substances from the encapsulated microcapsules, resulting in the formation of solid materials for coating repair. Qian *et al.* doped submicron particles of poly (3,4-ethylenedioxythiophene)/lignosulfonate (PEDOT/LS) into a mixture of 3,4-ethylenedioxythiophene (EDOT) and water to form a solid-stabilized Pickering emulsion.[167] The conductivity of the resulting PEDOT/LS complex prepared *via* Pickering emulsion polymerization was increased by two orders of magnitude. As a result, the surface resistance of glass coated with PEDOT/LS-PEP decreased from 1012 to 106 Ω sq^{-1}. These novel PEDOT/LS-PEP complexes effectively fulfill the requirements for industrial antistatic materials.

Yan *et al.* proposed a hybrid of $Ni(OH)_2$ and lignin sulfonate to synthesize micron-sized particles, which were utilized for the synergistic emulsification in oil spill adsorption at sea.[168] The co-emulsification process was facilitated by the electrostatic attraction between $Ni(OH)_2$ particles and oppositely charged SL, effectively mitigating the flocculation of $Ni(OH)_2$ in seawater. In comparison with individual emulsifiers such as $Ni(OH)_2$ particles or SL alone, the hybrid particles exhibited superior performance in producing smaller, more uniform, and highly stable oil–water emulsion droplets, enabling efficient adsorption of highly viscous crude oi. The utilization of Pickering emulsion systems for the development of lignin composites with other materials has emerged as a ubiquitous strategy in material design, thereby enhancing the functional attributes of emulsions. The study conducted by Li *et al.* presents a novel and facile approach for synthesizing antibacterial phase change microcapsules (micro-PCMs) decorated with silver particles, wherein CLPs served as both the Pickering stabilizer and the reducing agent for silver ions.[165] The results demonstrated that the shell of the micro-PCMs incorporated embedded lignin particles, which effectively reduced silver ions to form Ag/lignin micro-PCMs. These resulting Ag/lignin micro-PCMs exhibited a well-defined core–shell spherical morphology with a high phase-transition enthalpy of 177.6 J g^{-1}, excellent encapsulation efficiency of 69.0%, and remarkable thermal durability.

5. Challenges and prospects

The Pickering emulsion is a distinctive dispersion system stabilized by solid particles. The heterogeneous nature of

lignin, characterized by various chemical bonds formed by aromatic and phenolic units, enhances the amphiphilic structure of lignin and facilitates its enrichment into nanoparticles for application in emulsion systems. As an emerging emulsion stabilized by lignin nanoparticles, the CLPs-Pickering emulsion exhibits significant potential across multiple fields owing to its unique physicochemical properties; however, there remain several challenges that need to be addressed.[21] In terms of the dispersion mechanism of the emulsion, a single theory cannot comprehensively define all studies at present due to the diverse modification strategies employed for lignin nanoparticles resulting in different interface combinations. Before fully understanding the mechanism of interface interaction in this two-phase system, it is crucial to harness the stabilizing role of CLPs as polymer blend stabilizers and emphasize the functional characteristics of lignin such as antioxidant activity, antibacterial properties, and stability performance. This will enable biopolymers like lignin to realize their full potential for practical applications.

The first and foremost challenge faced by this technology lies in gaining a more detailed understanding of CLPs formation process. However, due to the varied chemical structures of lignin along with different extraction methods and sources used, development and utilization across a wider range of applications pose certain challenges. Ensuring consistent product properties especially regarding controlled formation of spherical nanoparticles becomes imperative for standardized production. From a fundamental research perspective, optimizing function of lignin nanomaterials through manipulation of particle size, wettability, shape anisotropy aggregation behavior, and surface chemistry presents various challenges that future researchers must focus on addressing. A more comprehensive understanding of how to effectively control these factors is a primary focus for future researchers. In order to achieve sustainable production of CLP-Pickering emulsions on a commercial scale, it is crucial to gain deeper insights into the underlying mechanisms. Specifically, it is important to determine the relative significance of interface stabilization by adsorption particles as true Pickering stabilizers compared to their contribution as functional modulators.

Furthermore, the field of CLPs faces additional challenges in terms of achieving faster, simpler, and more environmentally friendly production methods. Additionally, there is a need to explore new and/or combined applications that align with the concept of transforming waste into wealth. While CLPs offer numerous opportunities for high-value applications utilizing Pickering emulsion systems, there is still potential for further exploration. Consequently, various chemical modifications have been proposed to expand the potential uses of lignin in developing advanced lignin-based polymers and nanostructures. For example, esterification or alkylation can be employed to enhance compatibility between the lignin polymer and non-polar polymer matrices by targeting hydroxyl groups on the lignin structure. Another challenge lies in addressing the high polydispersity of lignin which complicates controlling its macromolecular structure after undergoing chemical modification. The emergence of nano-lignin based materials has enabled better control over the macromolecular structure of lignin, thereby enhancing properties of polymer blends and nanocomposites along with their biomedical applications.

However, it is important to acknowledge that while lignin itself demonstrates limited ecotoxicity, the modification and utilization of chemicals may lead to unintended consequences, such as undesired interactions with various molecules.[149] Moreover, due to the hindrance of phenolic hydroxyl groups, the biodegradability of modified lignin is also compromised, potentially impacting the environment. Extensive research is crucial for comprehending the potential toxicity, interactions, degradability, accumulation, and localization of nanoparticles in living organisms. Additionally, enhancing its photostability poses a significant challenge in harnessing lignin as an effective component in anti-ultraviolet agents. It can be argued that advancing Pickering emulsions for encapsulating and delivering bioactive compounds will continue to be a pivotal area of investigation; thus, envisioning breakthroughs through developing functionalized CLPs-Pickering emulsions with responsive stimulus capabilities.

The industrialization of CLPs-Pickering products is experiencing a significant upsurge in terms of industrial development. It is imperative to promptly initiate pilot trials and cultivate more sophisticated, application-oriented industrial production processes. The expeditious implementation of structural optimization for operational units and comprehensive economic evaluation throughout the entire cycle should be prioritized.

Author contributions

Conceptualization, C. H., W. Y., K. Z.; Writing – original draft, J. G.; Writing – review & editing, all authors; investigation, J. G.; Visualization, J. G.; Supervision, W. Y., C. H.; Funding acquisition, W. Y.

Data availability

Data availability is not applicable to this article as no new data were created or analyzed in this study.

Conflicts of interest

There are no conflicts to declare.

Acknowledgements

This work was supported by the Fundamental Research Funds of CAF (CAFYBB2021ZX001).

References

1 M. Zembyla, B. S. Murray and A. Sarkar, *Trends Food Sci. Technol.*, 2020, **104**, 49–59.
2 W. Ramsden and F. Gotch, *Proc. R. Soc. London*, 1904, **72**, 156–164.
3 S. U. Pickering, *J. Chem. Soc., Trans.*, 1907, **91**, 2001–2021.
4 L. E. Low, S. P. Siva, Y. K. Ho, E. S. Chan and B. T. Tey, *Adv. Colloid Interface Sci.*, 2020, **277**, 102117.
5 Y. Chevalier and M.-A. Bolzinger, *Colloids Surf., A*, 2013, **439**, 23–34.
6 Z. Wang and Y. P. Wang, *Materials*, 2016, **9**, 903.
7 C. Miesch, E. Pentzer and T. Emrick, in *Polymer Science: A Comprehensive Reference*, ed. K. Matyjaszewski and M. Möller, Elsevier, Amsterdam, 2012, ch. 7.15, vol. 7, pp. 287–311.
8 H. Jiang, Y. Sheng and T. Ngai, *Curr. Opin. Colloid Interface Sci.*, 2020, **49**, 1–15.
9 J. Texter, *Colloid Polym. Sci.*, 2022, **300**, 587–592.
10 V. Chaudhary and S. Sharma, *J. Polym. Res.*, 2019, **26**, 102.
11 G. J. Marshall, *US Pat*, 25949131947, 1947.
12 K.-D. Hungenberg, *Macromol. Chem. Phys.*, 2007, **208**, 1020–1020.
13 D. G. Ortiz, C. Pochat-Bohatier, J. Cambedouzou, M. Bechelany and P. Miele, *Engineering*, 2020, **6**, 468–482.
14 S. A. F. Bon, in *Particle-Stabilized Emulsions and Colloids: Formation and Applications*, ed. T. Ngai and S. A. F. Bon, The Royal Society of Chemistry, 2014, pp. 1–7.
15 V. Calabrese, J. C. Courtenay, K. J. Edler and J. L. Scott, *Curr. Opin. Green Sustain. Chem.*, 2018, **12**, 83–90.
16 C. Ji and Y. Wang, *Adv. Colloid Interface Sci.*, 2023, **318**, 102970.
17 C. Miao, S. Atifi and W. Y. Hamad, *Carbohydr. Polym.*, 2020, **248**, 116775.
18 S. Guo, X. Li, Y. Kuang, J. Liao, K. Liu, J. Li, L. Mo, S. He, W. Zhu, J. Song, T. Song and O. J. Rojas, *Carbohydr. Polym.*, 2021, **253**, 117223.
19 B. L. Pelegrini, F. M. B. Fernandes, T. Fernandes, J. H. de Oliveira, H. C. Rosseto, A. G. O. Junior, A. V. Reis, E. V. Castelani, F. N. C. Sobral, W. V. I. Shirabayashi, L. Benyahia, C. Chassenieux and M. M. de Souza Lima, *Cellulose*, 2021, **28**, 6201–6238.
20 X. Liu, M.-C. Li, B. Liao, S. Liu, K. Lu, K. Lv, J. Sun, C. Liu, C. Mei and Q. Wu, *Chem. Eng. J.*, 2023, **475**, 146372.
21 H. Dupont, V. Maingret, V. Schmitt and V. Héroguez, *Macromolecules*, 2021, **54**, 4945–4970.
22 N. Ghavidel and P. Fatehi, *ChemSusChem*, 2021, **14**, 4850–4877.
23 R. C. Sun, *ChemSusChem*, 2020, **13**, 4385–4393.
24 L. Bai, L. G. Greca, W. Xiang, J. Lehtonen, S. Huan, R. W. N. Nugroho, B. L. Tardy and O. J. Rojas, *Langmuir*, 2019, **35**, 571–588.
25 R. Rinaldi, R. Jastrzebski, M. T. Clough, J. Ralph, M. Kennema, P. C. A. Bruijnincx and B. M. Weckhuysen, *Angew. Chem., Int. Ed.*, 2016, **55**, 8164–8215.
26 S. Beisl, A. Friedl and A. Miltner, *Int. J. Mol. Sci.*, 2017, **18**, 2367.
27 K. Chen, S. Wang, Y. Qi, H. Guo, Y. Guo and H. Li, *ChemSusChem*, 2021, **14**, 1284–1294.
28 E. Lizundia, M. H. Sipponen, L. G. Greca, M. Balakshin, B. L. Tardy, O. J. Rojas and D. Puglia, *Green Chem.*, 2021, **23**, 6698–6760.
29 W. D. H. Schneider, A. J. P. Dillon and M. Camassola, *Biotechnol. Adv.*, 2021, **47**, 107685.
30 W. D. H. Schneider, A. J. P. Dillon and M. Camassola, *Biotechnol. Adv.*, 2021, **47**, 107685.
31 L. E. Low, K. C. Teh, S. P. Siva, I. M. L. Chew, W. W. Mwangi, C. L. Chew, B.-H. Goh, E. S. Chan and B. T. Tey, *Environ. Nanotechnol., Monit. Manage.*, 2021, **15**, 100398.
32 Y. Pang, Y. Sun, Y. Luo, M. Zhou, X. Qiu, C. Yi and H. Lou, *Ind. Crops Prod.*, 2021, **167**, 113468.
33 W. Zhang, J. Shen, P. Gao, Q. Jiang and W. Xia, *Ind. Crops Prod.*, 2022, **188**, 115651.
34 M. Stanisz, Ł. Klapiszewski, M. N. Collins and T. Jesionowski, *Mater. Today Chem.*, 2022, **26**, 101198.
35 J. Y. Xu, C. Y. Li, L. Dai, C. L. Xu, Y. D. Zhong, F. X. Yu and C. L. Si, *ChemSusChem*, 2020, **13**, 4284–4295.
36 Y. H. P. Zhang, *J. Ind. Microbiol. Biotechnol.*, 2008, **35**, 367–375.
37 L. Hu, T. Li and Y. Jing, *J. Phys. Chem. C*, 2024, **128**, 3832–3838.
38 P. F. O. Ferreira, A. L. S. Pereira, M. F. Rosa and R. S. de Santiago-Aguiar, *Ind. Crops Prod.*, 2022, **186**, 115119.
39 T. Yuan, J. Zeng, D. Guo, Q. Sun, B. Wang, L. Sha and K. Chen, *Int. J. Biol. Macromol.*, 2023, **224**, 1142–1151.
40 J. Gould, G. Garcia-Garcia and B. Wolf, *Materials*, 2016, **9**, 791.
41 H. Guo, X. Lu, Y. Yang, J. Wei, L. Wu, L. Tan, Y. Tang and X. Gu, *Mol. Catal.*, 2023, **540**, 113041.
42 M. R. Ridho, E. A. Agustiany, M. Rahmi Dn, E. W. Madyaratri, M. Ghozali, W. K. Restu, F. Falah, M. A. Rahandi Lubis, F. A. Syamani, Y. Nurhamiyah, S. Hidayati, A. Sohail, P. Karungamye, D. S. Nawawi, A. H. Iswanto, N. Othman, N. A. Mohamad Aini, M. H. Hussin, K. Sahakaro, N. Hayeemasae, M. Q. Ali and W. Fatriasari, *Adv. Mater. Sci. Eng.*, 2022, **2022**, 1363481.
43 V. K. Thakur, M. K. Thakur, P. Raghavan and M. R. Kessler, *ACS Sustainable Chem. Eng.*, 2014, **2**, 1072–1092.
44 X. Lu and X. Gu, *Int. J. Biol. Macromol.*, 2022, **205**, 539–552.
45 X. Shi, S. Gao, C. Jin, D. Zhang, C. Lai, C. Wang, F. Chu, A. J. Ragauskas and M. Li, *Green Chem.*, 2023, **25**, 5907–5915.
46 C. Frangville, M. Rutkevicius, A. P. Richter, O. D. Velev, S. D. Stoyanov and V. N. Paunov, *ChemPhysChem*, 2012, **13**, 4235–4243.
47 P. K. Mishra and A. Ekielski, *Nanomaterials*, 2019, **9**, 243.
48 S. Behera, S. Mohapatra, B. C. Behera and H. Thatoi, *Crit. Rev. Biotechnol.*, 2024, **44**, 774–794.

49 T. R. Pang, G. H. Wang, H. Sun, L. L. Wang, Q. M. Liu, W. J. Sui, A. M. Parvez and C. L. Si, *ACS Sustainable Chem. Eng.*, 2020, **8**, 9174–9183.
50 H. Li, Y. H. Deng, B. Liu, Y. Ren, J. Q. Liang, Y. Qian, X. Q. Qiu, C. L. Li and D. F. Zheng, *ACS Sustainable Chem. Eng.*, 2016, **4**, 1946–1953.
51 Y. Zhou, Y. M. Han, G. Y. Li, F. Q. Xiong and F. X. Chu, *Int. J. Biol. Macromol.*, 2020, **165**, 2136–2142.
52 F. Wang, J. Tang, H. Liu, G. Yu and Y. Zou, *Mater. Chem. Front.*, 2019, **3**, 356–364.
53 G. Colucci, A. Santamaria-Echart, S. C. Silva, L. G. Teixeira, A. Ribeiro, A. E. Rodrigues and M. F. Barreiro, *Colloids Surf., A*, 2023, **666**, 131287.
54 H. Cuthill, C. Elleman, T. Curwen and B. Wolf, *Foods*, 2021, **10**, 371.
55 J. Tian, J. Chen, P. Wang, J. Guo, W. Zhu, M. R. Khan, Y. Jin, J. Song and O. J. Rojas, *Green Chem.*, 2023, **25**, 3671–3679.
56 W. Zhao, B. Simmons, S. Singh, A. Ragauskas and G. Cheng, *Green Chem.*, 2016, **18**, 5693–5700.
57 R. Li, D. Huang, S. Chen, L. Lei, Y. Chen, J. Tao, W. Zhou and G. Wang, *Nanoscale*, 2022, **14**, 10299–10320.
58 J. Chen, Z. Pang, Y. Zhang, J. Chu, D. Zhang, X. Lu and C. Dong, *Bioresour. Technol.*, 2022, **343**, 126130.
59 F. Xiong, Y. Han, S. Wang, G. Li, T. Qin, Y. Chen and F. Chu, *Ind. Crops Prod.*, 2017, **100**, 146–152.
60 X. Zhao, J. Wang, K. Lan, Z. Zhao, C. Lai, C. Huang and Q. Yong, *ACS Sustainable Chem. Eng.*, 2024, **12**, 2871–2880.
61 P. Figueiredo, M. H. Lahtinen, M. B. Agustin, D. M. de Carvalho, S. P. Hirvonen, P. A. Penttila and K. S. Mikkonen, *ChemSusChem*, 2021, **14**, 4718–4730.
62 A. Czaikoski, A. Gomes, K. C. Kaufmann, R. B. Liszbinski, M. B. de Jesus and R. L. D. Cunha, *Ind. Crops Prod.*, 2020, **154**, 112762.
63 K. Gao, J. Liu, X. Li, H. Gojzewski, X. Sui and G. J. Vancso, *ACS Sustainable Chem. Eng.*, 2022, **10**, 9334–9344.
64 X. Li, J. Shen, B. Wang, X. Feng, Z. Mao and X. Sui, *ACS Sustainable Chem. Eng.*, 2021, **9**, 5470–5480.
65 L. Chen, S.-M. Luo, C.-M. Huo, Y.-F. Shi, J. Feng, J.-Y. Zhu, W. Xue and X. Qiu, *Green Chem.*, 2022, **24**, 285–294.
66 M. Ma, L. Dai, C. Si, L. Hui, Z. Liu and Y. Ni, *ChemSusChem*, 2019, **12**, 5239–5245.
67 M. R. V. Bertolo, L. B. Brenelli de Paiva, V. M. Nascimento, C. A. Gandin, M. O. Neto, C. E. Driemeier and S. C. Rabelo, *Ind. Crops Prod.*, 2019, **140**, 111591.
68 M. Lievonen, J. J. Valle-Delgado, M.-L. Mattinen, E.-L. Hult, K. Lintinen, M. A. Kostiainen, A. Paananen, G. R. Szilvay, H. Setälä and M. Österberg, *Green Chem.*, 2016, **18**, 1416–1422.
69 M. B. Agustin, P. A. Penttilä, M. Lahtinen and K. S. Mikkonen, *ACS Sustainable Chem. Eng.*, 2019, **7**, 19925–19934.
70 Z. Wei, Y. Yang, R. Yang and C. Wang, *Green Chem.*, 2012, **14**, 3230–3236.
71 R. Yin, L. Chen and L. Ma, *J. Sep. Sci.*, 2019, **42**, 3563–3570.
72 T. Lindströmn, *Colloid Polym. Sci.*, 1979, **257**, 277–285.
73 J. Tian, J. Chen, J. Guo, W. Zhu, M. R. Khan, Q. Fu, Y. Jin, H. Xiao, J. Song and O. J. Rojas, *Colloids Surf., A*, 2023, **670**, 131503.
74 S. S. Nair, S. Sharma, Y. Pu, Q. Sun, S. Pan, J. Y. Zhu, Y. Deng and A. J. Ragauskas, *ChemSusChem*, 2014, **7**, 3513–3520.
75 L. Matsakas, A. Karnaouri, A. Cwirzen, U. Rova and P. Christakopoulos, *Molecules*, 2018, **23**, 1822.
76 A. A. Yaqoob, S. H. Sekeri, M. B. H. Othman, M. N. M. Ibrahim and Z. H. Feizi, *Arabian J. Chem.*, 2021, **14**, 103182.
77 I. A. Gilca, V. I. Popa and C. Crestini, *Ultrason. Sonochem.*, 2015, **23**, 369–375.
78 M. N. Garcia Gonzalez, M. Levi, S. Turri and G. Griffini, *J. Appl. Polym. Sci.*, 2017, **134**, 45318.
79 H. Yin, L. Liu, X. Wang, T. Wang, Y. Zhou, B. Liu, Y. Shan, L. Wang and X. Lü, *Colloids Surf., A*, 2018, **545**, 51–59.
80 Y. Pang, Z. Qin, S. Wang, C. Yi, M. Zhou, H. Lou and X. Qiu, *Colloid Polym. Sci.*, 2020, **298**, 1001–1012.
81 W. Yang, F. Dominici, E. Fortunati, J. M. Kenny and D. Puglia, *Ind. Crops Prod.*, 2015, **77**, 833–844.
82 H. Trevisan and C. A. Rezende, *Ind. Crops Prod.*, 2020, **145**, 112105.
83 X. Yu, S. Chen, W. Wang, T. Deng and H. Wang, *J. Cleaner Prod.*, 2022, **339**, 130769.
84 M. Ago, S. Huan, M. Borghei, J. Raula, E. I. Kauppinen and O. J. Rojas, *ACS Appl. Mater. Interfaces*, 2016, **8**, 23302–23310.
85 N. Chen, L. A. Dempere and Z. Tong, *ACS Sustainable Chem. Eng.*, 2016, **4**, 5204–5211.
86 T. Zou, M. H. Sipponen and M. Osterberg, *Front. Chem.*, 2019, **7**, 370.
87 Z. Wei, Y. Yang, R. Yang and C. Wang, *Green Chem.*, 2012, **14**, 3230–3236.
88 A. Moreno, M. Morsali, J. Liu and M. H. Sipponen, *Green Chem.*, 2021, **23**, 3001–3014.
89 J. Liu, X. Shi, L. Ma, D. Zhang, C. Lai, C. Wang, M. Li, A. J. Ragauskas, F. Chu and Y. Xu, *Green Chem.*, 2023, **25**, 5428–5437.
90 M. H. Sipponen, M. Smyth, T. Leskinen, L.-S. Johansson and M. Österberg, *Green Chem.*, 2017, **19**, 5831–5840.
91 H. Yi, Y. Yang, X. Gu, J. Huang and C. Wang, *J. Mater. Chem. A*, 2015, **3**, 13749–13757.
92 C. G. Conner, A. N. Veleva, V. N. Paunov, S. D. Stoyanov and O. D. Velev, *Part. Part. Syst. Charact.*, 2020, **37**, 2000122.
93 W. Zhang, C. Y. Diao and L. Wang, *Biotechnol. Biofuels Bioprod.*, 2023, **16**, 55.
94 D. Tian, J. Hu, R. P. Chandra, J. N. Saddler and C. Lu, *ACS Sustainable Chem. Eng.*, 2017, **5**, 2702–2710.
95 S. Beisl, A. Miltner and A. Friedl, *Int. J. Mol. Sci.*, 2017, **18**, 1244.
96 A. A. Myint, H. W. Lee, B. Seo, W.-S. Son, J. Yoon, T. J. Yoon, H. J. Park, J. Yu, J. Yoon and Y.-W. Lee, *Green Chem.*, 2016, **18**, 2129–2146.

97 Z. Sun, X. X. Yan, Y. Xiao, L. J. Hu, M. Eggersdorfer, D. Chen, Z. Z. Yang and D. A. Weitz, *Particuology*, 2022, **64**, 153–163.
98 W. W. Zhao, B. Simmons, S. Singh, A. Ragauskas and G. Cheng, *Green Chem.*, 2016, **18**, 5693–5700.
99 Y. Z. Zhu and Q. Shen, *Abstr. Pap. Am. Chem. Soc.*, 2005, **230**, U1227–U1227.
100 N. Ghavidel and P. Fatehi, *ChemSusChem*, 2020, **13**, 4567–4578.
101 C. Hadjiefstathiou, A. Manière, J. Attia, F. Pion, P.-H. Ducrot, E. Gore and M. Grisel, *J. Mol. Liq.*, 2023, **390**, 123030.
102 C. Cai, X. Zhan, M. Zeng, H. Lou, Y. Pang, J. Yang, D. Yang and X. Qiu, *Green Chem.*, 2017, **19**, 5479–5487.
103 S. Li, J. A. Willoughby and O. J. Rojas, *ChemSusChem*, 2016, **9**, 2460–2469.
104 L. Dai, Y. Li, F. Kong, K. Liu, C. Si and Y. Ni, *ACS Sustainable Chem. Eng.*, 2019, **7**, 13497–13504.
105 Z. Shomali and P. Fatehi, *ACS Sustainable Chem. Eng.*, 2022, **10**, 16563–16577.
106 N. Hong, *J. Agric. Food Chem.*, 2022, **70**, 1196–1202.
107 A. M. Borrero-Lopez, L. Wang, H. Li, T. V. Lourencon, C. Valencia, J. M. Franco and O. J. Rojas, *Int. J. Biol. Macromol.*, 2023, **242**, 124941.
108 X. Shi, K. Wang, S. Gao, D. Zhang, C. Lai, C. Jin, M. Li, C. Wang, Q. Yong and F. Chu, *Ind. Eng. Chem. Res.*, 2023, **62**, 17765–17775.
109 J. Wang, Y. Fan, H. Wang, J. Yin, W. Tan, X. Li, Y. Shen and Y. Wang, *Chem. Eng. J.*, 2022, **430**, 132920.
110 Y. Pang, Y. Cheng, Y. Luo, C. Yi, M. Zhou and H. Lou, *J. Dispersion Sci. Technol.*, 2024, **45**, 1972–1980.
111 K. S. Silmore, C. Gupta and N. R. Washburn, *J. Colloid Interface Sci.*, 2016, **466**, 91–100.
112 X. Yu, X. Li, S. Ma, Y. Wang, W. Zhu and H. Wang, *Adv. Funct. Mater.*, 2023, **33**, 2214911.
113 S. A. Gundersen and J. Sjöblom, *Colloid Polym. Sci.*, 1999, **277**, 462–468.
114 M. Rayner, D. Marku, M. Eriksson, M. Sjöö, P. Dejmek and M. Wahlgren, *Colloids Surf., A*, 2014, **458**, 48–62.
115 T. E. Nypelo, C. A. Carrillo and O. J. Rojas, *Soft Matter*, 2015, **11**, 2046–2054.
116 M. Yu, H. Xin, D. He, C. Zhu, Q. Li, X. Wang and J. Zhou, *Int. J. Biol. Macromol.*, 2023, **238**, 123938.
117 M. Derakhshandeh, B. K. Pilapil, B. Workman, M. Trifkovic and S. L. Bryant, *Soft Matter*, 2018, **14**, 4268–4277.
118 M. S. Manga, T. N. Hunter, O. J. Cayre, D. W. York, M. D. Reichert, S. L. Anna, L. M. Walker, R. A. Williams and S. R. Biggs, *Langmuir*, 2016, **32**, 4125–4133.
119 B. K. Pilapil, H. Jahandideh, S. L. Bryant and M. Trifkovic, *Langmuir*, 2016, **32**, 7109–7116.
120 E. Vignati, R. Piazza and T. P. Lockhart, *Langmuir*, 2003, **19**, 6650–6656.
121 C. E. D. A. Padilha, C. D. C. Nogueira, S. C. B. Matias, J. D. B. D. Costa Filho, D. F. D. S. Souza, J. A. D. Oliveira and E. S. D. Santos, *Colloids Surf., A*, 2020, **603**, 125260.
122 O. Gordobil, N. Blazevic, M. Simonic and A. Sandak, *Int. J. Biol. Macromol.*, 2023, **233**, 123561.
123 S. Lu, D. Yang, M. Wang, M. Yan, Y. Qian, D. Zheng and X. Qiu, *Colloids Surf., A*, 2020, **585**, 124158.
124 A. M. Bago Rodriguez and B. P. Binks, *Curr. Opin. Colloid Interface Sci.*, 2022, **57**, 101556.
125 Y. Yang, Z. Wei, C. Wang and Z. Tong, *Chem. Commun.*, 2013, **49**, 7144–7146.
126 Z. Zhang, A. Mulyadi, X. Kuang, W. Liu, V. Li, P. Gogoi, X. Liu and Y. Deng, *Polym. Eng. Sci.*, 2018, **59**, 964–972.
127 A. Sarkar and E. Dickinson, *Curr. Opin. Colloid Interface Sci.*, 2020, **49**, 69–81.
128 N. Ghavidel and P. Fatehi, *Langmuir*, 2021, **37**, 3346–3358.
129 E. Kimiaei, M. Farooq, R. Grande, K. Meinander and M. Österberg, *Adv. Mater. Interfaces*, 2022, **9**, 2200988.
130 Q. Dai, Y. Bai, B. Fu and F. Yang, *ACS Omega*, 2023, **8**, 7430–7437.
131 Q. Zhao, L. Fan, J. Li and S. Zhong, *Food Hydrocolloids*, 2024, **146**, 109185.
132 I. Lugoloobi, X. Li, Y. Zhang, Z. Mao, B. Wang, X. Sui and X. Feng, *Int. J. Biol. Macromol.*, 2020, **165**, 3078–3087.
133 X. Li, N. Hegyesi, Y. Zhang, Z. Mao, X. Feng, B. Wang, B. Pukánszky and X. Sui, *Eur. Polym. J.*, 2019, **110**, 378–384.
134 M. B. Agustin, N. Nematollahi, M. Bhattarai, E. Oliaei, M. Lehtonen, O. J. Rojas and K. S. Mikkonen, *Cellulose*, 2023, **30**, 8955–8971.
135 K. Wang, M. Zhu, Z. Yang, L. Bai, S. Huan and C. Wang, *ACS Sustainable Chem. Eng.*, 2023, **11**, 9132–9142.
136 D. M. D. Carvalho, M. H. Lahtinen, M. Bhattarai, M. Lawoko and K. S. Mikkonen, *Green Chem.*, 2021, **23**, 9084–9098.
137 V. Ugartondo, M. Mitjans and M. P. Vinardell, *Bioresour. Technol.*, 2008, **99**, 6683–6687.
138 J. Ponomarenko, T. Dizhbite, M. Lauberts, A. Volperts, G. Dobele and G. Telysheva, *J. Anal. Appl. Pyrolysis*, 2015, **113**, 360–369.
139 T. Dizhbite, G. Telysheva, V. Jurkjane and U. Viesturs, *Bioresour. Technol.*, 2004, **95**, 309–317.
140 M. Azadfar, A. H. Gao, M. V. Bule and S. Chen, *Int. J. Biol. Macromol.*, 2015, **75**, 58–66.
141 S. Lv, S. Liang, J. Zuo, S. Zhang, J. Wang and D. Wei, *Iran. Polym. J.*, 2023, **32**, 1477–1497.
142 H. Xin, J. Xu, J. Zhou and X. Wang, *Waste Biomass Valorization*, 2024, **15**, 3651–3658.
143 Y. Bai, X. Li, X. Wang, X. Wang, X. Yang, H. Xin, D. Sun, J. Zhou and M. Chai, *Langmuir*, 2024, **40**, 554–560.
144 M. Lin, L. Yang, H. Zhang, Y. Xia, Y. He, W. Lan, J. Ren, F. Yue and F. Lu, *Ind. Crops Prod.*, 2021, **174**, 114212.
145 S. R. Yearla and K. Padmasree, *J. Exp. Nanosci.*, 2015, **11**, 289–302.
146 H. Trevisan and C. A. Rezende, *Ind. Crops Prod.*, 2020, **145**, 112105.
147 K. Chen, L. Lei, H. Lou, J. Niu, D. Yang, X. Qiu and Y. Qian, *Int. J. Biol. Macromol.*, 2020, **158**, 430–442.

148 K. Chen, L. Lei, Y. Qian, A. Xie and X. Qiu, *ACS Sustainable Chem. Eng.*, 2018, **7**, 810–818.
149 S. H. Sekeri, M. N. M. Ibrahim, K. Umar, A. A. Yaqoob, M. N. Azmi, M. H. Hussin, M. B. H. Othman and M. Malik, *Int. J. Biol. Macromol.*, 2020, **164**, 3114–3124.
150 K. Chen, Y. Qian, C. Wang, D. Yang, X. Qiu and B. P. Binks, *J. Colloid Interface Sci.*, 2021, **591**, 352–362.
151 B. Yan, G. Lu, R. Wang, S. Kang, C. Huang, H. Wu and Q. Yong, *Front. Chem. Sci. Eng.*, 2023, **17**, 976–989.
152 Y. Pang, X. Li, S. Wang, X. Qiu, D. Yang and H. Lou, *React. Funct. Polym.*, 2018, **123**, 115–121.
153 Y. Pang, S. Wang, X. Qiu, Y. Luo, H. Lou and J. Huang, *J. Agric. Food Chem.*, 2017, **65**, 11011–11019.
154 A. D. E. S. Pereira, J. Luiz de Oliveira, S. Maira Savassa, C. Barbara Rogério, G. Araujo de Medeiros and L. F. Fraceto, *J. Cleaner Prod.*, 2022, **345**, 131145.
155 R. Wen and S. Fu, *J. Wood Chem. Technol.*, 2022, **42**, 456–466.
156 M. J. Hasan, E. Westphal, P. Chen, A. Saini, I. W. Chu, S. J. Watzman, E. Urena-Benavides and E. S. Vasquez, *RSC Adv.*, 2023, **13**, 2768–2779.
157 H. Fan, Z. Zhang, M. Hou, J. Song, G. Yang and B. Han, *ACS Appl. Mater. Interfaces*, 2021, **13**, 25234–25240.
158 J. Liu, P. Xiu, Y. Zhu, K. Wang, S. Tong, Y. Ma, H. Guo and X. Gu, *Catal. Commun.*, 2024, **187**, 106868.
159 H. Guo, J. Zhao, Y. Chen, X. Lu, Y. Yang, C. Ding, L. Wu, L. Tan, J. Long, G. Yang, Y. Tang, N. Tsubaki and X. Gu, *ACS Catal.*, 2024, **14**, 703–717.
160 C. Tang, Y. Chai, C. Wang, Z. Wang, J. Min, Y. Wang, W. Qi, R. Su and Z. He, *Langmuir*, 2022, **38**, 12849–12858.
161 A. Moreno and M. H. Sipponen, *Nat. Commun.*, 2020, **11**, 5599.
162 Z. Cai, Y. Li, H. He, Q. Zeng, J. Long, L. Wang and X. Li, *Ind. Eng. Chem. Res.*, 2015, **54**, 11501–11510.
163 M. Gan, J. Pan, Y. Zhang, X. Dai, Y. Yin, Q. Qu and Y. Yan, *Chem. Eng. J.*, 2014, **257**, 317–327.
164 J. Pan, Y. Yin, M. Gan, M. Meng, X. Dai, R. Wu, W. Shi and Y. Yan, *Chem. Eng. J.*, 2015, **266**, 299–308.
165 X. Li, Y. Wang, B. Wang, X. Feng, Z. Mao and X. Sui, *Int. J. Biol. Macromol.*, 2020, **144**, 624–631.
166 Y. Wang, X. Li, C. Shen, Z. Mao, H. Xu, Y. Zhong, X. Sui, X. Feng and B. Wang, *Int. J. Biol. Macromol.*, 2020, **146**, 1–8.
167 Y. Qian, T. Wang, X. Qiu, D. Zhao, D. Liu and Y. Deng, *ACS Sustainable Chem. Eng.*, 2016, **4**, 7193–7199.
168 B. Yan, X. Wang, X. Zhang, S. Liu, M. Li and R. Ran, *J. Environ. Chem. Eng.*, 2021, **9**, 106607.

